The direct reaction mechanism at high energies

V. M. Kolybasov, G. A. Leksin, and I. S. Shapiro

Institute of Theoretical and Experimental Physics, Moscow

Usp. Fiz. Nauk **113**, 239–284 (June 1974)

On the basis of the current experimental data, a survey is given of our knowledge of the physical nature and mechanism of direct nuclear reactions—processes in which most of the energy and momentum of the incident particle is transferred to a single nucleon or to a relatively small group of nucleons. It is shown why it is particularly advantageous to make use of high-energy particles to investigate the nature of direct reactions. The interrelationship of nuclear physics and elementary particle physics is discussed. An outline is given of the theoretical fundamentals of the study of direct reactions. Consideration is given mainly to the determination of the mechanism of direct reactions involving three or more particles in the final state. The pole and triangle Feynman diagrams, as well as an approximate method of allowing for the contribution of other diagrams, are discussed in detail. The following types of reactions are considered: quasielastic processes, double charge exchange of pions, elastic *pd* scattering, the K-*d* interaction, and the nuclear capture of pions and kaons. The experimental data are analyzed and compared with the theoretical results. Desirable directions of further experimental investigations are indicated.

CONTENTS

I. INTRODUCTION

Direct nuclear reactions include those processes in which most of the energy and momentum of the incident particle is transferred to a single nucleon or to a relatively small group of nucleons. As a result, one observes fast particles that are correlated with the direction of the incident beam, and weakly excited (or completely unexcited) residual nuclei. Protons and composite particles show up in many direct processes in the same way. An example is provided by knock-out reactions like (p, pd), (p, pα) and (α, 2α), in which the kinematic picture is similar to that of a free-particle collision and does not differ in any way from that of the processes (p, 2p) or (p, pn).

Practically all known direct reactions are now interpreted in terms of a "direct-interaction" picture, i.e., a direct collision of the incident particle with a small group of nucleons which leave the nucleus. Investigations of recent years have shown, however, that, in spite of the naive ideas which prevailed quite recently, it is not a simple matter to test the direct-interaction hypothesis. The solution of this problem is related to a number of contemporary problems of nuclear physics.

A number of experimental investigations of direct nuclear reactions are considered in detail in certain reviews [1-6], which, however, are devoted mainly to the prospects of obtaining spectroscopic information on the positions and properties of nuclear levels.

The aim of the present paper is to examine, on the basis of the current experimental data, the state of our knowledge of the physical nature and mechanism of direct reactions. This problem has been discussed earlier in the review literature (see [7-19]), but the experimental data and theoretical results which have appeared since then necessitate a fresh examination of the problem.

The new ideas that have been introduced in the study of direct nuclear reactions in the past five years are connected mainly with the utilization of high-energy particles and with methodological progress in the technique of multi-dimensional analysis of the data. This has made it possible to carry out a number of informative experiments that are dictated by current theoretical ideas.

1. Why high energies?

High energies are of interest in studying the nature of direct reactions for the following reasons:

a) The possibility of transferring small momenta and high energies extends the boundaries of the physical region and allows one to examine the dependence of the amplitudes within a much greater range of variation of the kinematic variables than at low energies. This makes it possible to observe the irregularities (whose scale is determined by the value of the binding energy of the particles in the nucleus) that are characteristic of the mechanism under consideration. In certain cases, one can come closer to the singular points of the reaction amplitude, where the mechanism for the process shows up more clearly. Moreover, at high energies it is possible to transfer large excitation energies to the nucleus without significantly suppressing the reaction probabilities. (This required small momentum transfers, $q \lesssim 1/R$, where R is the radius of the nucleus.)

b) One enlarges the diversity of particles which take part in the reaction. The utilization of meson beams makes it possible to realize reactions involving different charge states of the incident and final particles un-

der practically identical kinematic conditions. This circumstance is important for the determination of reaction mechanisms, as well as for the study of nuclear structure. Direct reactions of pion capture play a special role in the study of the dynamical correlation of the nucleons in nuclei.

Reactions involving the virtual production of nucleon or hyperon isobars, which take place when high-energy particles collide with nucleons inside the nucleus, constitute an additional source of information about the relation between the nuclear process as a whole and the "elementary event", owing to the characteristic energy dependence of its amplitude (a baryon resonance may be, as it were, an indicator of a direct process).

c) Current ideas about the nature of direct processes assume their universality (with respect to the scale of energies). A proof of this would be given by a description of high-energy cross sections in terms of the nuclear constants (reduced widths) measured in experiments at low energies.

2. Plan of the review

In what follows, we shall be concerned mainly with the determination of the mechanism of those direct reactions in which there are three or more particles in the final state. The point is that one must carry out a complex investigation (the measurement and comparison with the theory of a large number of characteristics of a reaction) to identify the mechanism. From this point of view, it is a simpler problem to identify the mechanisms of reactions involving three final particles than to ascertain the mechanism of a binary reaction from the experimental data. This is so because of the large number of independent kinematic variables, as a consequence of which the theoretical predictions are richer. In particular, the various symmetries that are peculiar to the simplest diagrams show up more clearly; secondly, there appear moving complex singularities of the amplitude, which lead to characteristic irregularities in the behavior of the cross section as a function of the kinematic variables. This will be demonstrated below for the case of two simple mechanisms: the pole and the "triangle" mechanism [1]. We shall consider the following class of reactions: quasi-elastic processes (knock-out reactions), reactions described by the triangle mechanism (double charge exchange of pions, pd elastic scattering, and the K^--deuteron interaction), and the nuclear capture of pions and kaons. The theoretical foundations of the study of direct reactions are outlined in Chap. II. We describe in detail the characteristics corresponding to the pole and triangle Feynman diagrams, as well as an approximate method of allowing for the contribution of other diagrams. This is followed by an analysis of the experimental data and their comparison with the theoretical ideas: in Chap. III for quasi-elastic processes, in Chap. IV for reactions described by the triangle mechanism, and in Chap. V for the capture of pions and kaons.

II. THEORETICAL FOUNDATIONS

Current ideas about the nature of direct processes can be reduced briefly to the following [7,8]. The nucleus is a dynamical system which virtually emits and reabsorbs all possible particles. These virtual particles, which are emitted for a very short time, 10^{-21}–10^{-23} sec (of the order of the duration of the direct reaction), form the periphery of the nucleus in the same way that virtual pions form the periphery of a nucleon, the particles which are the least bound to the nucleus being the most "peripheral." A direct process is the result of the collision of the incident particle with one or with several virtual particles. This collision causes a nuclear reaction in which some of the products may be captured, with the formation of a residual nucleus, while the others are emitted externally.

A formalism which is adequate for this picture is the Feynman-diagram technique, which, from the very beginning, incorporates all particles, including nucleons and more complex structures like deuterons and α particles, on an equal footing. In the diagrammatic language, direct processes correspond to graphs with a small number of internal lines (i.e., virtual particles), and the idea of a reaction mechanism acquires a precise meaning in accordance with the diagram which gives the dominant contribution to the rapidly varying part of the reaction amplitude [2].

The special advantage of the diagrammatic technique is that it enables us to avoid the use of nuclear wave functions. Generally speaking, the system "relativistic particle + nucleus" has no wave function, since new particles can be produced. The system "relativistic particle + nucleon" has no potential. In the traditional formalism of direct processes, one must make new adjustments for all these attributes whenever new mechanisms are introduced. In the diagrammatic method, the basic concept of the theory is not the wave function, but the amplitude for a real or virtual process. The amplitude for a process always exists. In a direct process, the amplitude for a reaction on a nucleus is expressed in terms of the amplitude for an elementary event.

Another significant virtue of the diagrammatic language is its generality. It enables us to describe a wide range of nuclear reactions and to follow the analogy with processes involving the interactions of elementary particles.

1. The pole mechanism (single-particle exchange)

It is meaningful to consider some particular diagram individually only in that region of the kinematic variables in which it is distinguished from the remaining diagrams; as a rule, this is the region near the singularity of the diagram in question. The pole diagram of Fig. 1 has a singularity in the variable t_{AB}, which is related to the momentum transfer from the target nucleus A to the residual nucleus B:

$$t_{AB} = -(\mathbf{p}_A - \mathbf{p}_B)^2 + 2(m_A - m_B)(E_A - E_B) = -\frac{m_A}{m_B} q^2, \qquad (2.1)$$

this singularity is at the point $t^0_{AB} = 2m_{iB}\epsilon$; here p, E and m are the momenta, kinetic energies and masses, q is the momentum of the nucleus B in the laboratory system, m_{iB} is the reduced mass of particles i and B, and ϵ is the binding energy of particles i and B in the nucleus A, given by $\epsilon = m_B + m_i - m_A$ [3]. As a rule, this

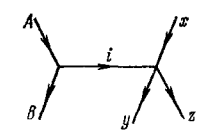

FIG. 1. The pole diagram corresponding to the reaction A + x → B + y + z.

singularity of the amplitude is the closest one to the physical region for the reaction

$$A + x \to B + y + z \tag{2.2}$$

in the variable t_{AB} (the physical region for the three-body reaction (2.2) is determined by the condition $t_{AB} \leq 0$). We may therefore expect that, in a number of cases, the pole diagram of Fig. 1 will give the main contribution in the region of small momentum transfers ($q < 100-150$ MeV/c) to the amplitudes for processes such as the (p, 2p), (p, pd) and (π, πN) quasi-elastic knock-out reactions, as well as reactions like (π^+, 2p), (π^-, nγ), (p, πd), etc. The problem of how to test the validity of the foregoing statement is the main content of this subsection.

a) **The pole diagram.** The amplitude for the reaction (2.2) corresponding to the diagram of Fig. 1 can be expressed in terms of the amplitude Γ for the decay

$$A \to B + i \tag{2.3}$$

and the amplitude M′ for the reaction

$$i + x \to y + z \tag{2.4}$$

as follows:

$$M^{\mu_B\mu_y\mu_z}_{\mu_A\mu_x} = \frac{2m_i m_B}{m_A} \frac{1}{q^2+\varkappa^2} \sum_i \Gamma^{\mu_B\mu_i}_{\mu_A} (M')^{\mu_y\mu_z}_{\mu_i\mu_x}; \tag{2.5}$$

here $\varkappa = (2m_{Bi}\epsilon)^{1/2}$, and μ_k is the spin projection of the k-th particle in the z-axis. It is convenient to extract the spin dependence in the quantity $\Gamma^{\mu_B\mu_i}_{\mu_A}$ in an explicit form and expand it in invariant form factors F, which are functions of t_{AB} alone (or, equivalently, functions of the relative momentum of particles i and B, which coincides with q)[18,20]:

$$\Gamma^{\mu_B\mu_i}_{\mu_A} = 2\pi \left(\frac{\varkappa}{2m^2_{Bi}}\right)^{1/2} \sum_{l,J} \gamma_{lJ} F_{lJ}(q) \sum_{\mu m} C^{J\mu}_{j_i\mu_i j_B\mu_B} C^{j_A\mu_A}_{J\mu l m} Y_{lm}(\mathbf{n}_{iB}). \tag{2.6}$$

The quantities J and μ have the interpretation of the total spin of particles i and B (the channel spin) and its projection, l, the orbital angular momentum of the relative motion of particles i and B in the nucleus A, and n_{iB} is a unit vector in the direction of the relative momentum of these particles. By virtue of the conservation of spatial parity, the expansion (2.6) contains either only even l (if the product of the intrinsic parities of the particles A, B and i is +1) or only odd l (if this product is −1). The $F_{lJ}(q)$ are form factors characterizing the momentum distribution of the virtual particles, normalized by the condition $F_{lJ}(i\varkappa) = 1$. For small $q \lesssim 1/R$, where, strictly speaking, it is meaningful to consider only the pole approximation (R is the channel radius, i.e., the minimum distance between the particles i and B for which their relative motion may be regarded as free or determined entirely by the Coulomb interaction), the structure of the form factor is determined mainly by the quantity R, and a good approximation is provided by the so-called Butler form factor [8], which corresponds to allowance for the wave function of the relative motion of particles i and B only for $r > R$. The Butler form factors are independent of the channel spin. We quote their forms for $l = 0$ and 1:

$$F_0(q) = e^{-\varkappa R}\left(\cos qR + \frac{\varkappa}{q}\sin qR\right),$$
$$F_1(q) = -i\left(1+\frac{1}{\varkappa R}\right)e^{-\varkappa R}\left\{\sin qR + \frac{(\varkappa R)^2}{1+\varkappa R}\left[\frac{\sin qR}{(qR)^2} - \frac{\cos qR}{qR}\right]\right\}. \tag{2.7}$$

We note that $F_l(q) \sim (qR)^l$ for $qR \ll 1$.

The constants γ_{lJ}, known as the reduced vertex parts, determine the probability of the decay (2.3). If the decay were actually possible, its probability would be given by $\lambda = |\gamma|^2 Q$, where Q is the energy release in the process (2.3) and $\gamma^2 = \Sigma_{l,J}\gamma^2_{lJ}$. In using the Butler form factors, we have the following relation between γ^2 and the dimensionless reduced width θ^2 that is employed in nuclear spectroscopy [8,21]

$$\gamma^2_{lJ} = \frac{6\theta^2_{lJ}}{(\varkappa R)^3 |h^{(1)}_l(i\varkappa R)|^2}, \tag{2.8}$$

where R is the channel radius, and $h^{(1)}_l$ is the spherical Hankel function of the first kind (or the singular solution of the Coulomb problem, if the particles are charges) [4].

The amplitude M′ can also be expanded in invariant amplitudes which depend only on the invariant variables t_{xz} (defined in analogy with (2.1)), s_{yz} (to within a factor, coinciding with the energy of particles y and z in their c.m.s.) and, generally speaking, since particle i is virtual, on the square of the 4-momentum of this particle (which is uniquely related to t_{AB})[18,20,23]. The corresponding formulas are given in Appendix I. To illustrate the spin structure of the pole diagram, we also give there a graphical scheme for summing the Clebsch-Gordan coefficients [24] that occur in evaluating $|\overline{M}|^2$, the square of the modulus of the matrix element, summed over the spin states of the final particles and averaged over the spin states of the initial particles:

$$\overline{|M|^2} = \frac{1}{(2j_A+1)(2j_x+1)} \sum_{\mu_A,\mu_x,\mu_B,\mu_y,\mu_z} |M^{\mu_B\mu_y\mu_z}_{\mu_A\mu_x}|^2. \tag{2.9}$$

With the normalization which we have chosen for the amplitude and with allowance for the laws of conservation of energy and momentum, the differential cross section for the reaction (2.2) with unpolarized particles is related to $|\overline{M}|^2$ by the equation

$$\frac{d^3\sigma}{d\Omega_z\, d\Omega_y\, dE_y}\Big|_{\text{lab}} = \frac{\omega_B\omega_y\omega_x}{(2\pi)^5 p_x} \frac{\mathbf{p}^2_z p_y}{|p_z(\omega_x-\omega_0)/\omega_z - p_x z_{xz} - p_y z_{yz}|} \overline{|M|^2}; \tag{2.10}$$

here $d\Omega_z$ and $d\Omega_y$ are the elements of solid angle for the final particles, z_{xz} and z_{yz} are the cosines of the corresponding angles, ω_0 is the total energy of the colliding particles, and ω_B, ω_x, ω_y and ω_z are the total energies of the corresponding particles in the laboratory system. The problem of how to express the other experimentally observable characteristics in terms of $|\overline{M}|^2$ is considered in detail in the review [25]. In Appendix II we quote a number of formulas which express $d\sigma/dq$, $d\sigma/dp_z$, etc., in terms of the differential cross section for the reaction (2.4).

b) **Cases in which the cross sections factorize.** In the case of unpolarized particles, the amplitude for the reaction (2.2) factorizes in the pole approximation, i.e., it can be represented as a product of two factors, one of which refers to the left-hand vertex of the diagram of Fig. 1 and depends only on t_{AB}, while the other is the amplitude for the virtual reaction (2.4) and is a function of t_{xz}, s_{yz} and t_{AB} (t_{AB} appears because of the dependence of this amplitude on the square of the 4-momentum of the transferred particle i). Thus, the amplitude depends on only three invariant variables, while in the general case the number of such variables is five for the five-point function (one may add, for example, s_{Ax} and s_{By}, which are related to the energy of the initial particles and the relative energy of particles B and y). This circumstance leads to an isotropic distribution in the Treiman-Yang angle (see below). Moreover,

the cross section for the process (2.4) appears simply as a factor in the cross section for the reaction (2.2).

In the general case of particles with spin, the summation over the spin states of the virtual particle in Eq. (2.5) leads to a breakdown of factorization, and the probability for the reaction (2.2) does not reduce to a product of the probabilities of the virtual processes $A \to B + i$ and $i + x \to y + z$. However, if the virtual particle i is nonrelativistic (for this, particle B must be nonrelativistic in the laboratory system, and the binding energy of particle i in the nucleus A must be much less than the mass of this particle), then there exists a wide class of reactions for which $\overline{|M|^2}$ factorizes [20]. In this case $\overline{|M'|^2}$, the square of the modulus of the amplitude for the reaction (2.4), averaged over the spin states, appears as a factor [5]:

$$\overline{|M|^2} = \frac{2\pi\varkappa}{(q^2+\varkappa^2)^2} |\gamma_{lJ}|^2 |F_{lJ}(q)|^2 \overline{|M'|^2}. \qquad (2.11)$$

$\overline{|M'|^2}$ in turn is related to the differential cross section $d\sigma_0/d\Omega$ for the reaction $i + x \to y + z$ [6]:

$$\left.\frac{d\sigma_0}{d\Omega}\right|_{\text{c.m.}} = \frac{m_i m_x m_y m_z}{(2\pi)^2 (\omega_y + \omega_z)^2} \frac{p_y}{p_i} \overline{|M'|^2}, \qquad (2.12)$$

where all quantities refer to the c.m.s. of particles y and z.

Thus, just as in the spinless case, the differential cross section for the reaction (2.2) contains the cross section for the reaction (2.4) as a factor. Let us list the cases in which the square of the modulus of the amplitude factorizes:

1) The spin of the virtual particle, j_i, is 0 or 1/2. In the case when the spin of the transferred particle is 1, $\overline{|M|^2}$ factorizes [27] if the quadrupolarization of particle i is small in the inverse reaction of (2.4), namely $y + z \to i + x$. We stress that $\overline{|M|^2}$ no longer factorizes if the virtual particle i has spin 1/2 but is relativistic, since the effect of relativistic spin flip appears when transforming from the laboratory system (i.e., the center-of-mass system of the reaction $A \to B + i$) to the c.m.s. of the process (2.4).

2) The main contribution in the vertex corresponding to the decay $A \to B + i$ comes from the form factor associated with zero orbital angular momentum of the relative motion of particles B and i ($l = 0$).

3) The main contribution in the vertex $A \to B + i$ comes from the state with $J = 0$ or 1/2 (we recall that J is the total spin of particles B and i).

Factorization holds in the foregoing cases even when the particles x, y and z at the right-hand vertex are relativistic. However, if all the particles which take part in the reaction are nonrelativistic, we have the following additional cases of factorization:

4) Only the terms with the total spin of particles i and x (j_{ix}) equal to 0 or 1/2 are important in the expansion of the amplitude for the reaction (2.4) in the invariant amplitudes (see Eq. (A.1) of Appendix I).

5) Only the terms with $L = 0$ are important in the same expansion (this corresponds to the absence of a spin-orbit interaction).

c) **Program for the identification of the pole mechanism.** To establish the pole mechanism, one must compare the experimental data with a number of theoretical distributions that are characteristic of this mechanism. We shall list below the experimental measurements that are desirable.

A number of the features which are characteristic of the pole mechanism are connected with the fact that the form factor of the process (2.3) and the pole denominator distinguish small values of $q \sim 1/R$, $\sqrt{2m_i\epsilon}$. Consequently, in distributions such as that in the momentum of one of the fast particles at a fixed angle or in the angle between two outgoing fast particles, maxima are observed at points corresponding to the kinematics of the reaction (2.4) on free particles i. However, the form of such dependences depends essentially on the dynamics of the processes (2.3) and (2.4), especially on the structure of the form factor $F_{lJ}(q)$, and may in principle be similar to that which is given by other diagrams [11]. As we shall see below (see Chap. III), such dependences are not very crucial.

We shall begin the discussion of the program of identifying the pole mechanism with a criterion which is independent of the specific form of the amplitudes for the virtual processes. This is:

1) The Treiman-Yang criterion. In the cases of factorization enumerated above, $\overline{|M|^2}$ depends only on the variables t_{AB}, t_{xz} and s_{yz}. Let us transform to the anti-laboratory system (i.e., the system in which $p_x = 0$). We shall denote the momenta of particles in this system by primed variables. It is easy to see that the invariants t_{AB}, t_{xz} and s_{yz} are unaltered if the (p'_y, p'_z) plane is rotated about the direction of the momentum of the virtual particle:

$$p'_i = p'_A - p'_B = p'_y + p'_z. \qquad (2.13)$$

Thus, $\overline{|M|^2}$ is also unchanged under such a rotation, i.e., the distribution must be isotropic in the Treiman-Yang angle φ [28], defined as the angle between the (p'_y, p'_z) and (p'_A, p'_B) planes [7].

The Treiman-Yang criterion is applicable to a wide class of reactions such as (p, pN), (p, pα) and (π, πN), as well as reactions on nuclei A in which the residual nucleus B and the pole particle i are in an s state, and also certain other processes [20,30]. As we shall see in Chap. III, this criterion is one of the most sensitive ones.

The Treiman-Yang rotation is in fact equivalent to an azimuthal rotation in the c.m.s. of the reaction $i + x \to y + z$, and the isotropy of the distribution in the Treiman-Yang angle reflects the azimuthal symmetry of this reaction. If none of the foregoing conditions for factorization are satisfied but the amplitude is dominated by the pole diagram, then the square of the modulus of the matrix element turns out to be a polynomial in $\cos\varphi$, and an upper bound on the degree r of this polynomial can be specified [31]:

$$r \leqslant \min\{2l, [J], [j_i], [j_{ix}], 2L\},$$

where $[j] = 2j$ for integral j and $2j - 1$ for half-integral j; the quantity L is introduced in Eq. (A.1) of Appendix I.

Invariance with respect to a reflection in the plane formed by the momenta of particles A, B and i in the anti-laboratory system implies that the distribution in the Treiman-Yang angle must be symmetric with respect to $\varphi = 0$, independently of which diagrams describe the reaction amplitude.

Like all the other criteria, the Treiman-Yang cri-

terion is a necessary, but not a sufficient, condition for the pole mechanism. It is difficult to give a general answer to the question as to how convincingly isotropy of the distribution in the Treiman-Yang angle indicates that the contribution of all diagrams other than the pole diagram is small. The simple theoretical estimates that have been made so far [32], on the basis of the study of triangle diagrams and the interference between the pole and triangle mechanisms, indicate that an admixture of mechanisms other than the pole mechanism generally leads to an appreciable breakdown of the isotropy in the distribution in φ (one must consider those kinematic regions in which the relative energies in all three pairs of final particles are not very small). The existing experimental data (see Chap. III) also indicate that the Treiman-Yang criterion is very sensitive to the reaction mechanism. Nevertheless, a reliable determination of the mechanism requires a check of several further predictions of the theory.

2) Dependence of the differential cross section on the momentum of the residual nucleus. The pole mechanism enables us to predict the dependence of the cross section on the momentum of the residual nucleus. As we have already mentioned, it distinguishes small q. The cross section falls off sharply when q is greater than the characteristic momentum q_0 of particle i in the nucleus A ($q_0 \sim \sqrt{2m_i\epsilon}$, $1/R$). At $q=0$, the matrix element has a maximum if $l=0$ and vanishes if $l \neq 0$. However, other diagrams may also give such a behavior in principle [11], so that even a pronounced q-dependence cannot in itself constitute a demonstration of the pole mechanism of a reaction.

3) Distribution in the polar angle of the residual nucleus. The amplitude corresponding to the pole diagram of Fig. 1 gives at small q a completely determined distribution in the polar angle at which the residual nucleus is emitted. (Examples of this type, as well as other theoretical distributions, will be demonstrated in Chap. III.) The study of $(\pi^-, \pi^- p)$ reactions on C^{12} and Li^6 has shown that this distribution is very sensitive to an admixture of other mechanisms.

4) Dependence of the cross section on the initial energy. If one of the cases of factorization applies, then $\overline{|M|^2}$ is independent of the initial energy. Thus, by measuring the differential cross section at various initial energies but fixed values of the invariants t_{AB}, t_{xz} and s_{yz}, we may test this consequence of the pole mechanism. There have so far been no such experiments in the domain of nuclear reactions.

5) Absolute value of the differential cross section. In the pole approximation, the cross section for the reaction (2.2) is expressed in terms of the probability of the virtual decay $A \to B+i$ and the cross section for the reaction (2.4). The $A \to B+i$ decay probability can be determined independently by studying other direct reactions whose diagrams contain the same nuclear vertex, such as a stripping or pick-up reaction. The cross section for the reaction (2.4) can be taken from experiments involving free particles. There is another possible way of testing the hypothesis that the pole diagram has a dominant role. It often turns out to be convenient to carry out such a test by comparing the reduced widths obtained from data on different reactions or from data on a single reaction at different energies. It seems that such an analysis was first performed for the reaction $C^{12}(\pi^-, \pi^- n)C^{11}$ in [33] (see also [34]). Specific examples are given in Chap. III.

6) Measurement of the cross section for the reaction $A+x \to B+y+z$ as a function of the independent kinematic invariants of the reaction $i+x \to y+z$. The differential cross section for the first reaction must duplicate the behavior of the cross section for the reaction $i+x \to y+z$. For example, a resonant behavior of the cross section for the reaction (2.4) leads to a resonance maximum in the cross section for the reaction (2.2) [33] 8). Here we can note a characteristic such as the momentum distribution of one of the fast secondary particles at a fixed angle. If the reaction (2.4) takes place on a free particle i, this distribution has the form of a δ-function. For quasi-elastic scattering, the peak is broadened and shifted towards lower energies (see, e.g., [35]). As we have already pointed out above, such distributions depend strongly on the dynamics of the reaction (2.4) and the decay (2.3) and are apparently not very sensitive to the mechanism (we shall discuss this point in detail in Chap. III).

7) Polarization effects. A number of further possibilities occur in experiments involving polarized nuclei or the measurement of the polarization of the secondary particles [11,27,36,37]. One may expect polarization phenomena to be more sensitive to the reaction mechanism than other characteristics, making it easier to detect an admixture of any other mechanism in addition to the basic one. The point is that the basic mechanism (for example, the pole diagram) often leads to a vanishing polarization and asymmetry, and the polarization effects are then determined by its interference with the additional terms or simply by the additional terms.

The polarization and quadrupolarization of the fast particles y and z or the asymmetry in the production of these particles in reactions involving a polarized beam of particles x are, in their general form, the same as for the reaction $i+x \to y+z$, but taking place with particle i in some special polarized state (which is determined by the properties of the vertex for the virtual decay $A \to B+i$ [27]). However, in the above-mentioned cases in which $\overline{|M|^2}$ factorizes, the situation becomes simpler, and the foregoing polarization effects should be the same in the pole approximation as for the reaction $i+x \to y+z$ with free particles.

A number of predictions can be made about the asymmetry in the reaction (2.2) with a polarized target and the polarization of the residual nuclei. In a large number of cases, these quantities can be expressed in terms of the polarization P_i of particle i in the inverse reaction of (2.4), namely

$$y + z \to i + x. \tag{2.14}$$

This will be the case, for example, if one of the conditions for the factorization of $\overline{|M|^2}$ is satisfied and if the virtual decay $A \to B+i$ is described entirely by a single invariant form factor. Let us introduce the concept of asymmetry for a reaction involving the production of three particles. Let $\sigma_\uparrow$ and $\sigma_\downarrow$ be the differential cross sections for the reaction (2.2) when p_B, p_y and p_z are fixed, but with values P_A and $-P_A$ of the polarization of the target nucleus, and let σ_0 be the cross section on an unpolarized target. We shall define the asymmetry $\mathcal{A}$ as the ratio

$$\mathcal{A} = \frac{\sigma_\uparrow - \sigma_\downarrow}{2\sigma_0} \tag{2.15}$$

We shall quote the results for two of the simplest cases. Let $l=0$. Then

$$\mathcal{A}=3\left[\frac{(2j_i+1)\,j_i}{(j_i+1)}\,\frac{(2j_A+1)\,j_A}{(j_A+1)}\right]^{1/2}(-1)^{j_i+j_A+j_B}\begin{Bmatrix}1 & j_i & j_i\\ j_B & j_A & j_A\end{Bmatrix}(\mathbf{P}_A\mathbf{P}_i) \tag{2.16}$$

For example, when $j_i=1/2$,

$$\mathcal{A}=\begin{cases}-(\mathbf{P}_A\mathbf{P}_i), & \text{if } j_B=j_A-1/2,\\ \frac{j_A}{j_A+1}(\mathbf{P}_A\mathbf{P}_i), & \text{if } j_B=j_A+1/2,\end{cases} \tag{2.17}$$

For arbitrary l, but with $j_i=1/2$, the asymmetry can be expressed in terms of the quantities $(\mathbf{P}_A\cdot\mathbf{P}_i)$ and $(\mathbf{P}_i\cdot\mathbf{n}_{iB})(\mathbf{P}_A\cdot\mathbf{n}_{iB})$, where $\mathbf{n}_{iB}$ is a unit vector in the direction of the motion of particles i and B. More complex cases are analyzed in [27]. The foregoing discussion is also applicable to reactions of the type (e,ep). However, owing to the small polarization in ep scattering, a polarized electron beam is also required. There is so far no experimental information on polarization effects in three-particle reactions. The study of polarization phenomena can not only yield information about the reaction mechanism, but also allows a determination of the quantum numbers of the residual nucleus. This is of special interest in connection with the indications of the existence of highly excited nuclear states (the excitation energy reaches 50–70 MeV for S^{32} and Ca^{40}) from the data on (p, 2p) and (e, ep) reactions [38,39]. These states are interpreted as $(1s)^{-1}$ and $(1p)^{-1}$ hole levels. To confirm this interpretation, it is important to know the quantum numbers of the levels. One can hardly expect to obtain the necessary information by studying other reactions. Moreover, it is not possible to ascertain the nature of the observed maxima (whether they actually correspond to nuclear levels) without at the same time establishing the reaction mechanism. Our understanding of this problem could be greatly advanced by carrying out the program outlined above.

8) Test of isotopic relations. If several three-particle reactions are described by the pole mechanism, the nuclear vertices of the corresponding diagrams being identical, and if there exist isotopic-type relationships among the cross sections for the processes corresponding to the right-hand vertex of the diagram in Fig. 1, then these conditions imply a definite relationship among the cross sections for the original reactions.

Such a test has been carried out experimentally [40] for reactions of the type $(\pi, \pi N)$ in the vicinity of the Δ_{33} resonance. The total cross sections for the two-body reactions at the resonance energy satisfy the relationship

$$\frac{\sigma(\pi^-n\to\pi^-n)}{\sigma(\pi^+n\to\pi^+n)+\sigma(\pi^+n\to\pi^0p)}=3. \tag{2.18}$$

The analogous ratio for the corresponding quasi-elastic processes is expected to be somewhat smaller. For example, it was shown in [34] that the ratio of the total cross section for the reaction $C^{12}(\pi^-, \pi^-n)C^{11}$ to the sum of the cross sections for the reactions $C^{12}(\pi^+, \pi^+n)C^{11}$ and $C^{12}(\pi^+, \pi^0p)C^{11}$ should be 2.5–2.6. The reason for this is that, owing to the motion of the nucleons inside the nucleus, the cross section for the reaction (2.2) at a fixed initial energy involves the cross sections for the process (2.4) at various relative energies of particles y and z [33]. The contribution of the isospin-1/2 state of the πN system then becomes appreciable, and this leads to a reduction in the value of (2.18).

For the reactions $C^{12}(\pi, \pi N)C^{11}$, it has been found experimentally that the ratio in question has a value close to unity [40]. This indicates that, despite the fact that the data on the resonance behavior of the excitation curve for the reaction $C^{12}(\pi^-, \pi^-n)C^{11}$ [41] are in good agreement with calculations in the pole approximation [36] 9), there is an appreciable contribution from mechanisms other than the pole mechanism (the two-stage process $\pi^-C^{12}\to\pi^-C^{12*}$, $C^{12*}\to C^{11}+n$ [34,40,43] or charge exchange of the knock-out neutrons [44] are possible)—which is another confirmation of the fact that agreement with calculations on one or two characteristics is not sufficient to establish any particular reaction mechanism! At the same time, the experimental value of the ratio of the cross sections for the reactions $Be^9(\pi^-, \pi N)Li^8$ and $Be^9(\pi^+, \pi^+p)Li^8$ [40] is very close to the calculated value [34]. The agreement is also much better for the shape of the excitation curve. We may expect the contribution of non-pole mechanisms to be much smaller in this case.

As we have already pointed out, the realization of the program which we have outlined requires the execution of experiments in which all the independent kinematic variables of the reaction are measured. In this case, it is desirable to have the means of isolating a definite state of the residual nucleus, which requires a resolution in the excitation energy of the order of 1 MeV. It is therefore preferable to study reactions on light nuclei, which have a greater spacing between the low-lying levels. It is also desirable to achieve statistical reliability of the distribution in the Treiman-Yang angle for different ranges of variation of variables such as the momentum of the residual nucleus, the relative energy of particles y and z, and the momentum transferred from x to z. The same also applies to other distributions (for example, in the polar angle of the residual nucleus or in the momentum of a fast secondary particle at fixed angle).

To conclude the discussion of the pole mechanism, we note that the frequently encountered claim that knock-out reactions can provide information about the momentum distribution of the nucleons in the nucleus is hardly justified; at small momentum transfers, the behavior of the differential cross section is determined by the binding energy and the nuclear radius and provides practically nothing as a test of dynamical models; at large momentum transfers, however, as we shall see below, the pole mechanism ceases to be dominant, as a consequence of which the momentum distribution of the residual nuclei is no longer directly related to the momentum spectrum of the nucleons inside the nucleus.

2. The triangle diagram

In a direct process, the incident particle interacts with a particle which is virtually emitted from the nucleus. A reaction takes place, whose products either leave the nucleus (this corresponds to the pole diagram of Fig. 1) or take part in an (elastic or inelastic) interaction with the residual nucleus or with any of the constituents of this nucleus. The simplest diagram corresponding to the second variant is a triangle diagram such as that of Fig. 2a. Thus, the first fact which establishes the importance of studying the triangle diagram is that we must always deal with this diagram when secondary processes are considered. In particular, the singularity structure and the behavior of the various kinematic quantities determined by the reaction mech-

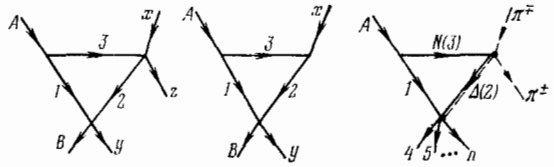

FIG. 2. Triangle diagrams for a three-body reaction (a), a binary reaction (b), and the isobar mechanism of double charge exchange of pions (c).

anism are important in extracting information on the characteristics of these secondary processes. This information is unique in a number of cases (for example, if the secondary process in question is nn scattering or a reaction involving an unstable particle).

Certain classes of nuclear reactions are definitely two-stage processes, since the quantum numbers cannot change in the required way for a single interaction. An example is the double charge exchange of pions at low energies. Here again the triangle mechanism is the simplest one.

The kinematic distributions corresponding to the diagram of Fig. 2a are generally less distinguished than those of the pole diagram of Fig. 1. The distribution in the momentum of the nucleus B, while limited to small momenta, is still usually much broader than that for the diagram of Fig. 1 and is more difficult to separate from the distributions given by more complex graphs. The distributions are not so clearly distinguished in the polar angle of the residual nucleus, in the Treiman-Yang angle (this distribution has a complex non-polynomial form [32]), in the momentum of the fast particle z, etc. [10]. It is clear from these considerations that it is difficult to identify the triangle mechanism. We note that, if there exist characteristic singularities in the elementary processes

$$3 + x \to 2 + z \tag{2.19}$$

and

$$1 + 2 \to B + y, \tag{2.20}$$

then they will also be reflected in the amplitude for the process as a whole, which will facilitate the determination of the mechanism. For example, a resonance behavior of the cross section for the reaction (2.20) would lead to a maximum in the distribution of events of the reaction (2.2) in E_{By}, the relative energy of particles B and y (the Migdal-Watson effect in the final-state interaction), but the shape and width of this maximum will also be determined by the singularities of the diagram of Fig. 2a itself.

However, in the problem of identifying the triangle mechanism, there occurs a very important circumstance, which was hitherto absent. The point is that the triangle diagram leads to moving complex singularities in the amplitude for the reaction (2.2) [45,46]. For a definite choice of the range of variation of the momenta of the particles participating in the reaction, these singularities come close to the physical region, thereby producing characteristic irregularities in the behavior of the differential cross sections, by which the reaction mechanism can be recognized [47]. The diagram of Fig. 2a has a square-root singularity in the energy E_{By} (a "cusp" in the cross section), as well as a logarithmic singularity whose position depends on the variable t_{xz}, the square of the momentum transferred from x to z. This second singularity leads to a characteristic maximum in the cross section as a function of the energy E_{By}, and the position and shape of this maximum vary with t_{xz}. The above-mentioned movement of the singularity can be detected by experimentally determining the differential cross section as a function of E_{By} at various values of t_{xz}. To do this, it is necessary to be able to vary E_{By} in the wide range from 0 to ~100 MeV (the upper limit of variation of E_{By} must be much greater than the characteristic nuclear binding energies) for small momentum transfers $t_{xz} \ll m^2$, where m is the nucleon mass. These conditions can be satisfied only for incident particles of high energy.

a) **The formalism.** The amplitude corresponding to the diagram of Fig. 2a can be expressed in terms of the amplitude for the decay of the nucleus A into the virtual particles 1 and 3, which we shall denote by Γ, and the amplitudes for the virtual processes (2.19) and (2.20), which will be denoted by M_1 and M_2. In accordance with the general rules [7,8]

$$(M_\Delta)^{\mu_B\mu_y\mu_z}_{\mu_A\mu_x} = -\frac{i}{2\pi^4} m_1 m_2 m_3 \times \sum_{\mu_1,\mu_2,\mu_3} \int \frac{\Gamma^{\mu_1\mu_3}_{\mu_A}(M_1)^{\mu_2\mu_z}_{\mu_3\mu_x}(M_2)^{\mu_B\mu_y}_{\mu_1\mu_2}\, dp_1\, dE_1}{(p_1^2 - 2m_1E_1 - i\eta)(p_2^2 - 2m_2E_2 - i\eta)(p_3^2 - 2m_3E_3 - i\eta)}. \tag{2.21}$$

The rather complex spin structure of this expression can be seen more clearly by making use of the representation of the amplitudes Γ, M_1 and M_2 in terms of invariant amplitudes (which is analogous to (2.6)) and a graphical scheme for summing the Clebsch-Gordan coefficients. Such formulas are given in Appendix II.

As a rule, the amplitude M_Δ does not factorize, and $\overline{|M_\Delta|^2}$ does not simply contain $\overline{|M_1|^2}$ and $\overline{|M_2|^2}$ as factors. Such a situation holds only in exceptional cases; one of the instances will be considered below in Chap. IV. Moreover, there is usually no simple relationship between the scalar amplitudes for the reaction as a whole and the scalar amplitudes for the "elementary" processes (2.19) and (2.20). This is so, not only because of the complex spin structure, but also because of the integration contained in Eq. (2.21).

There can be a simple relationship between the amplitudes only if one of the amplitudes M_1 or M_2 has a weak dependence on its variables and can be removed from the integral sign in (2.21); in addition, strong restrictions are imposed on the spins of the virtual particles and the orbital angular momenta at the vertices [18].

If we may neglect the presence of spin for the virtual particles, as well as the dependences of Γ, M_1 and M_2 on their natural variables, regarding these quantities as constants, then the integral (2.21) can be evaluated [45,47]. It is convenient to write the expression for M_Δ in terms of dimensionless variables ξ and λ defined as follows:

$$\xi = \frac{m_2}{m_3}\,\frac{m_A}{m_B + m_y}\,\frac{E_{By} - Q}{\varepsilon}, \tag{2.22}$$

$$\lambda = \frac{m_1}{m_3}\,\frac{2(m_x - m_z)(E_{By} - Q_0) - t}{2(m_B + m_y)\varepsilon}, \tag{2.23}$$

where

$$\left.\begin{aligned} \varepsilon &= m_1 + m_3 - m_A, \\ Q &= m_1 + m_2 - m_B - m_y, \\ Q_0 &= m_A + m_x - m_B - m_y - m_z, \\ E_{By} &= E_B + E_y - [(\mathbf{p}_y + \mathbf{p}_B)^2/2(m_y + m_B)] \end{aligned}\right\} \tag{2.24}$$

the last quantity being the energy of particles B and y

in their center-of-mass system, and

$$t = -(\mathbf{p}_x - \mathbf{p}_z)^2 + 2(m_x - m_z)(E_x - E_z).$$

The variable ξ may be either negative or positive in the physical region of the reaction (2.2). The variable λ can be expressed in terms of the momenta of particles x and z in the laboratory system:

$$\lambda = \frac{m_2^2 (\mathbf{p}_x - \mathbf{p}_z)^2}{2(m_1 + m_2)^2 m_{13}\varepsilon}, \qquad (2.25)$$

and is always greater than zero (provided that the initial nucleus A is stable).

In the variables ξ and λ, the expression for the reaction amplitude has the form

$$M_\Delta = C f_\Delta(\xi, \lambda), \qquad (2.26)$$

where the constant C includes Clebsch-Gordan coefficients depending on the spin projections of the initial and final particles, and

$$f_\Delta(\xi,\lambda) = \frac{1}{\sqrt{\lambda}} \ln \frac{\sqrt{\xi} - \sqrt{\lambda} + i}{\sqrt{\xi} + \sqrt{\lambda} + i} = \begin{cases} \frac{1}{\sqrt{\lambda}} \left[\ln \frac{(\sqrt{\xi} - \sqrt{\lambda})^2 + 1}{(\sqrt{\xi} + \sqrt{\lambda})^2 + 1} + i \operatorname{arctg} \frac{2\sqrt{\lambda}}{\xi - \lambda + 1} \right], & \text{if } \xi \geqslant 0, \\ \frac{2i}{\sqrt{\lambda}} \operatorname{arctg} \frac{\sqrt{\lambda}}{1 + \sqrt{-\xi}}, & \text{if } \xi < 0, \end{cases} \qquad (2.27)$$

the arctg function being defined in the range from 0 to π.

The function f_Δ has two singularities in the variable ξ: a square-root branch point $\xi = 0$ (a normal threshold) and a logarithmic branch point

$$\xi_\Delta = \lambda - 1 + 2i\sqrt{\lambda}. \qquad (2.28)$$

As a function of λ, the quantity f_Δ has only one singularity – a logarithmic branch point

$$\lambda_\Delta = \xi - 1 + 2i\sqrt{\xi}. \qquad (2.29)$$

We note that the function $f_\Delta(\xi, \lambda)$ is universal–it is the same for all reactions, since it is independent of the masses of the participating particles.

Equation (2.27) is also useful for describing the amplitude for a binary reaction (Fig. 2b) [48,49]. In this case, λ is defined as

$$\lambda = \frac{m_1}{m_3} \frac{m_x (E_{By} - Q_0)}{(m_B + m_y)\varepsilon}, \qquad (2.23a)$$

and λ and ξ are no longer independent variables, but can be expressed in terms of each other; M_Δ is in essence a function of only the initial energy.

b) **The case of an unstable virtual particle.** The virtual particles in the triangle diagram considered above may be not only nucleons or the lightest nuclei, but also baryon resonances. As an example, we cite the possible reaction mechanism of double charge exchange of pions, considered in [50], which corresponds to the diagram of Fig. 2c. The virtual reaction in this case is the process $\pi^\pm + N \to \Delta_{33}(1236) + \pi^\mp$, and one of the virtual particles is the $\Delta_{33}(1236)$ isobar. (The results of the experimental work [51] provide evidence that processes involving isobar production in the double charge exchange of high-energy pions play a significant role.)

The instability of the virtual particle (for definiteness, let it be particle 2) is taken into account by adding to its mass an imaginary part related to the resonance width Γ: $m_2 \to M_2 - i\Gamma/2$, and a corresponding replacement $m_2^2 \to m_2^2 - im_2\Gamma$ in the propagator of particle 2 written in a relativistically covariant form. This leads to the replacement

$$\xi \to \xi + i\rho, \qquad (2.30)$$

where

$$\rho = \frac{m_{12}\Gamma}{2m_{13}\varepsilon}. \qquad (2.31)$$

Thus, ξ, which we shall encounter below, is a real quantity, being defined by Eq. (2.22), in which m_2 should be interpreted as the real part of the mass of particle 2. The variable λ is not changed in any way by the introduction of a complex part in the mass of particle 2. Now

$$f_\Delta = \frac{1}{\sqrt{\lambda}} \left\{ \frac{1}{2} \ln \frac{(1+A)^2 + (\sqrt{\lambda} - B)^2}{(1+A)^2 + (\sqrt{\lambda} + B)^2} + i \operatorname{arctg} \frac{2(1+A)\sqrt{\lambda}}{(1+A)^2 + B^2 - \lambda} \right\}, \qquad (2.32)$$

where again $0 \leq \operatorname{arctg} x < \pi$, and the quantities A and B are defined as follows: for $\xi \geq 0$

$$B = \sqrt{\frac{-\xi + \sqrt{\xi^2 + \rho^2}}{2}}, \quad A = \frac{\rho}{2B}, \qquad (2.33a)$$

and for $\xi < 0$

$$A = \sqrt{\frac{-\xi + \sqrt{\xi^2 + \rho^2}}{2}}, \quad B = \frac{\rho}{2A}. \qquad (2.33b)$$

It is easy to see that Eq. (2.32) reduces to (2.27) when $\Gamma = 0$.

These relations are also applicable to the amplitude for a binary reaction $A + x \to B + y$ if the expression (2.23a) is used for λ.

The amplitude for the reaction (2.20) may have its own singularities in the energy (i.e., in ξ). If particle 2 is an isobar, it is possible that it (like the nucleon) has a resonant interaction with the nucleus, forming a compound system – a multi-baryon resonance ("isonucleus") with an excitation energy and width of the order of the isobar values [50,52] [11]. This would lead to a specific ξ-dependence of the amplitude [50], whose experimental observation would be one of the methods of deciding whether "isonuclei" exist.

c) Allowance for the nuclear form factor. The approximation in which the form factor corresponding to the nuclear decay $A \to 1 + 3$ is assumed to be constant is not always a good one, especially for $l \neq 0$ (where l is the relative orbital angular momentum of particles 1 and 3). Since both particles 1 and 3 are off the mass shell, the form factor Γ depends, in general, on two variables. However, in a potential model, there remains, as in Chap. II.1, a dependence on only the single variable p, the relative momentum of particles 1 and 3.

This dependence in the triangle diagram of Fig. 2a is most readily taken into account by transforming to the coordinate representation [12]. Let us introduce the wave function corresponding to the form factor $\Gamma_l(p)$:

$$\psi(r) = \frac{1}{(2\pi)^{3/2}} \int_0^\infty \frac{\Gamma_l(p)\, j_l(pr)\, p^2}{p^2 + \varkappa^2}\, dp. \qquad (2.34)$$

If the amplitudes for the virtual reactions (2.19) and (2.20) are assumed to be constant, as before, then the amplitude corresponding to the triangle diagram of Fig. 2c takes the form

$$M_\Delta = C' Y_{lm}(\hat{\mathbf{q}}) \int_0^\infty \psi(r)\, j_l(\sqrt{\lambda}\varkappa r) \exp(i\sqrt{\xi}\varkappa r)\, r\, dr \quad (\text{if } \xi \geqslant 0), \qquad (2.35a)$$

$$M_\Delta = C' Y_{lm}(\hat{\mathbf{q}}) \int_0^\infty \psi(r)\, j_l(\sqrt{\lambda}\varkappa r) \exp(-\sqrt{-\xi}\varkappa r)\, r\, dr \quad (\text{if } \xi < 0); \qquad (2.35b)$$

here $\mathbf{q} = \mathbf{p}_X - \mathbf{p}_Z$ ($\mathbf{p}_X$ and $\mathbf{p}_Z$ are the momenta in the laboratory system), and a cap over a variable denotes a

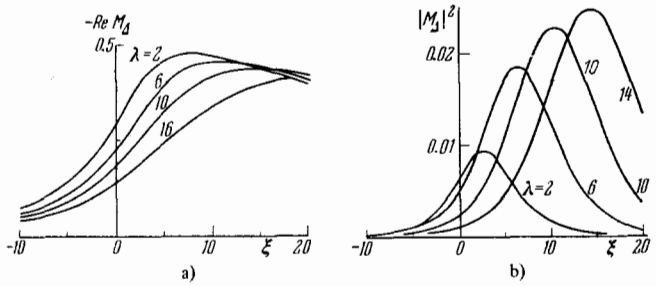

FIG. 3. Re M_Δ as a function of ξ for the case of a constant form factor (a), and $|M_\Delta|^2$ as a function of ξ for the double charge-exchange reaction on C^{12} with allowance for the nuclear form factor (b).

unit vector. The constant C' implicitly contains the Clebsch-Gordan coefficient associated with $Y_{lm}(\hat{q})$. The positive values are taken for the quantities $\sqrt{\lambda}$, $\sqrt{\xi}$ (for $\xi \geq 0$) and $\sqrt{-\xi}$ (for $\xi < 0$); j_l is a spherical Bessel function.

Equation (2.27) for the case of constant vertices is obtained from (2.35) if $l = 0$ and $\psi(r)$ is replaced by its asymptotic expression $\psi(r) = e^{-\kappa r}/r$.

If one of the virtual particles is unstable (let it be particle 2, as before), the expressions (2.35) remain valid, but we must make the substitution $\sqrt{\xi} \to iA + B$ in (2.35a), where A and B are given by (2.33).

To illustrate the picture of the moving singularities, Fig. 3a shows $\mathrm{Re}\, M_\Delta$ as a function of ξ for various values of λ, calculated using a constant form factor (this calculation was made for the double charge-exchange reaction on the nucleus C^{12}, which corresponds to the diagram of Fig. 2c, in accordance with which $\Gamma = 120$ MeV and $\rho = 4.9$) [54]. Figure 3b shows the ξ-dependence of $|M_\Delta|^2$ for various values of λ, calculated in this case with allowance for the form factor at the $C^{12} \to C^{11} + p$ vertex (a Gaussian form factor with $l = 1$ was adopted) [54]. The movement of the maxima of the curves is clearly seen in both figures. If detected experimentally, this would provide evidence for an appreciable contribution from the triangle diagram. However, this would clearly require an extremely accurate experiment.

Some applications of triangle diagrams in describing direct nuclear reactions and a comparison with the experimental data will be reported in Chap. IV.

d) **Relation to the Schrödinger formalism.** Many calculations carried out in the traditional Schrödinger formalism using wave functions correspond to allowance for the simplest triangle diagrams [55,56]. We may cite, as examples, the impulse approximation for elastic scattering, replacement reactions, the second iteration of the Faddeev equations for the reaction $p + d \to p + p + n$, etc. In particular, the impulse approximation for elastic scattering (or single scattering in the Glauber approximation) is equivalent to the triangle diagram in which the fast incident particle is scattered by one of the nucleons of the nucleus.

Most of the theoretical calculations of quasi-elastic knock-out reactions, as well as stripping and pick-up reactions, have been carried out in the plane-wave or distorted-wave impulse approximation, which corresponds to allowance for the pole diagram and the triangle diagrams involving elastic rescattering in the initial and final states [56,57]. Such calculations are hardly well-founded, since they make no allowance for either multiple scattering or the large number of graphs involving inelastic processes (one example is provided by the diagrams which involve an intermediate nucleus in an excited state, where this excitation is eliminated in the secondary interaction). Thus, there are many graphs that are not taken into account, whose singularities in the momentum transfer lie as far from the physical region as those of the triangle diagrams in the distorted-wave method. In other words, the triangle diagrams involving elastic rescattering are not distinguished in any way.

A more consistent method of taking into account the contribution of all the diagrams other than some prominent one will be outlined below.

3. Allowance for the contribution of more complex diagrams

Even if we are in the kinematic region near the singularity of a certain diagram, we cannot in general say that this diagram gives the main contribution. The contribution of other (usually more complex) diagrams may turn out to be important here. Sometimes this situation is favored by additional circumstances. For example, if the nuclear form factor corresponds to $l \neq 0$ in a pole diagram which is prominent in the region of small momenta q of the residual nucleus, then this diagram vanishes at $q = 0$, and the entire amplitude at this point is determined by the contribution of more complex diagrams.

However, in the case in which the singularity of the diagram in question is much closer than the singularities of other diagrams, we can usually say that it gives the main contribution to the rapidly varying part of the amplitude. This leads to the following method of analysis, which is more consistent than the distorted-wave method and, at the same time, more general, simpler, and at least as informative [7,47,58] [13]: considering a sufficiently narrow range of variation of the kinematic variables, we take into account explicitly the diagrams which dominate the rapidly varying part of the amplitude (what is implied is the variation in that variable in which the singularities of these diagrams are the nearest ones); the contribution of all the remaining diagrams, being a slowly varying function of this variable, is approximated by a complex constant, which must be chosen to give the best fit to the experimental data.

In carrying out the foregoing program, allowance must be made for the fact that the particles which participate in the reaction have spin, and the correction term must have the correct spin structure. We must therefore expand the amplitude in a set of independent spin tensors [18,60] and take the invariant form factors in this expansion to be constants. In the general case, the amplitude for the reaction (2.2) contains $(2j_A + 1)(2j_B + 1)(2j_X + 1)(2j_Y + 1)(2j_Z + 1)$ invariant form factors, each of which provides one complex free parameter in the calculations. Since the errors on the existing experimental results do not permit us to introduce a large number of free parameters, we must artificially reduce the number of invariant amplitudes employed in the calculations. For example, in one work [58] concerned with the theoretical analysis of (p, 2p) reactions at small momentum transfers, the spin structure of the correction term was chosen to have the same form as for the triangle diagram involving rescattering of one of the protons (after which the amplitude was of course ap-

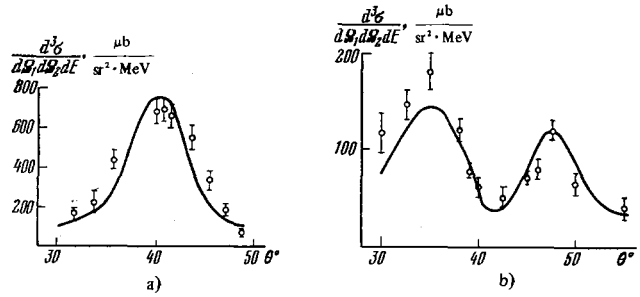

FIG. 4. Comparison of the theoretical predictions with the experimental data on the (p, 2p) reactions on He^4 at 460 MeV (a) and on Li^7 at 185 MeV (b) [58].

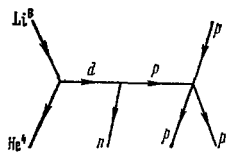

FIG. 5

propriately antisymmetrized with respect to the outgoing protons) [14]. One free complex parameter appeared in these calculations. All the remaining parameters were determined from different experiments (the main diagram was, of course, the pole diagram).

The procedure outlined above makes it possible to give a satisfactory description of the data on (p, 2p) reactions for all the nuclei that we have considered, except Li^6 (the case of Li^6 is discussed below). In Fig. 4 we show the results for He^4 (at 460 MeV) and Li^7 (at 185 MeV), together with the experimental data. The values of the reduced widths obtained from the analysis of (p, 2p) reactions are, as a rule, in agreement with the analogous quantities obtained from reactions of the type (n, d), (p, d) or (π, πN).

While the differential cross sections are not very sensitive to the spin structure of the slowly varying part of the amplitude, there is quite a different situation regarding polarization effects and the distribution in the Treiman-Yang angle. The first attempts to analyze polarization phenomena and the distribution in the Treiman-Yang angle with allowance for the non-pole "background" were made in [18,32,37]. A number of further applications of the method that we have described are considered in Chap. IV.

The main contribution to the rapidly varying part of the amplitude does not always come from a simple pole diagram like that of Fig. 1, even in the region of small momentum transfers. For example, as we have already mentioned, the analysis of Li^6(p, 2p) reactions in which allowance was made for the pole diagram and a "background" in the form of a constant does not provide a satisfactory description of the experimental data (an analysis based on the distorted-wave method leads to the same conclusion): if one studies the distribution in the scattering angle of the protons in the symmetric coplanar case (see Chap. III), the theory predicts a deep minimum at an angle in the region 80–85°, whereas this minimum is quite shallow experimentally. However, there are grounds for supposing that, owing to the instability of the He^5 nucleus produced in the reaction in question, there can be a large contribution from events

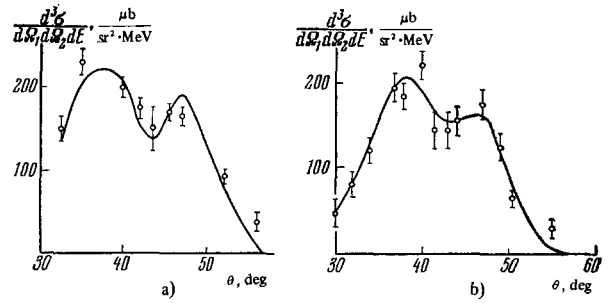

FIG. 6. Angular distributions for the reaction Li^6(p, 2p) at 155 (a) and 185 MeV (b) [61].

involving the three-body decay $Li^6 \rightarrow He^4 + p + n$ of the initial nucleus [15]. The simplest model is the diagram of Fig. 5. If allowance is made for this diagram [61], it is possible to achieve a marked improvement in the description of the data on the angular distribution (Fig. 6) and mutual agreement between the values of the reduced proton width of the Li^6 nucleus obtained from different reactions (see Chap. III).

III. QUASI-ELASTIC PROCESSES (EXPERIMENT)

1. Experiments of the simplest type

Experimental high-energy nuclear physics came into being together with the first experiments using relativistic accelerators about 20 years ago. The experimental arrangements that were used to investigate elastic pp scattering also made it possible to study the quasi-elastic process. Measurements were made of either a) the distribution in the scattering angle between the two protons [62] (in the case of elastic pp scattering, the scattering angle is close to 90°) or b) the momentum spectrum of the protons at a fixed angle [63,64]. As an example of the results, we show in Fig. 7, taken from the paper of Chamberlain and Segrè [62], the distribution in the scattering angle between the two protons that are produced when lithium nuclei are bombarded with 345-MeV protons. A maximum is clearly seen in the vicinity of the peak for elastic pp scattering, but it is displaced somewhat with respect to the precise position of the peak and has a width which exceeds that associated with the resolution of the experimental arrangement (the latter is indicated by the solid curve).

Other processes have also been studied in variant b), in particular (γ, π^+n) [65] and (e, ep) [66], as well as the knock-out of light nuclei. The first experiment in which outgoing deuterons were observed was performed in Dubna [67a] in 1956, immediately after the detection of elastic pd scattering at an angle close to 180° [67b]. Measurements were made of the spectrum of secondary particles ejected at 7.6° from D, Li, Be, C and O targets bombarded by 675-MeV protons. Figure 8 shows the spectrum of positive particles ejected from a lithium target. The peak for elastic pLi scattering is clearly seen. The high-momentum component of the spectrum obtained after subtracting the background (see the inset) is of special interest. This component results mainly from deuterons and has a maximum whose position coincides almost exactly with the expected position of the peak for elastic pd scattering. In other words, we see a typical picture of quasi-elastic scattering by deuterons "inside the nucleus" [16].

Subsequently, an improved experimental technique

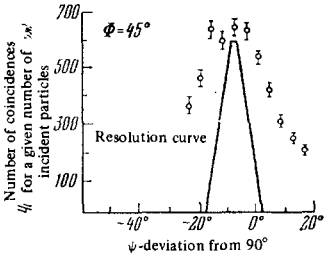

FIG. 7

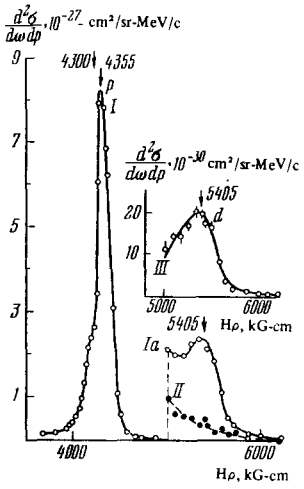

FIG. 8

FIG. 7. The number of events as a function of the difference between the scattering angle of the detected protons and the expected angle for elastic pp scattering. (p, 2p) reaction on a lithium target. E = 345 MeV [62].

FIG. 8. The spectrum of positive particles emerging at 7.6° from a lithium target exposed to protons with E = 675 MeV [67]. The dashed curve shows the background of protons. The inset shows the deuteron spectrum.

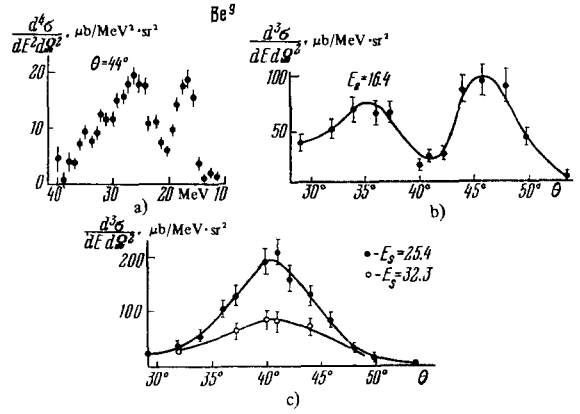

FIG. 9. The energy spectrum of the residual nucleus in the reaction $Be^9(p, 2p)B^8$ (a) and the distributions of the number of reaction events as a function of the angle between the protons in three ranges of the excitation energy (b and c).

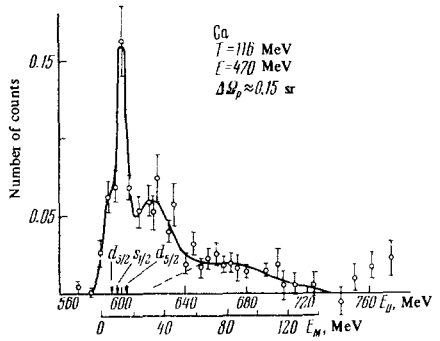

FIG. 10. The spectrum of excitation energies of the residual nucleus in the reaction $Ca^{40}(e, ep)$ [39].

was used to study the spectra of deuterons from (p, pd) reactions at 1 GeV on the nuclei He^4, Li^6, C^{12}, O^{16} and Pb [69] and at 670 MeV on a large group of nuclei from Li^6 to Pb in recent Dubna experiments [70]. In Chap. IV.2 we shall return to the results of recent experiments in which both (p, pd) and (p, π^+d) processes were observed.

It should be noted that the cross section for deuteron knock-out is relatively small. The cross sections for the knock-out of heavier fragments are still smaller (see [71]).

The data discussed in this subsection have played a major role in the formulation of current ideas about the nucleus. In particular, they have compelled us to take the virtual particles emitted by the nuclei to be not only nucleons, but also deuterons, tritium nuclei, etc. Moreover, the experiments of the simplest type are inadequate as a test of current theory. As we have already mentioned, we require for this purpose experiments in which all the independent kinematic variables are measured.

2. "Two-track" experiments

Such experiments were begun in 1957 with an investigation of (p, 2p) reactions at 185 MeV [72]. They involve measurements of the energies and scattering angles of the two fast particles, and this enables one to calculate all the characteristics of the residual nucleus.

Most of the experiments were originally aimed at the study of nuclear properties: the energy levels of the residual nucleus and the orbital angular momenta of the knock-out particles. This essentially spectroscopic problem determined the details of a number of experiments. These experiments were generally arranged in the so-called coplanar symmetric geometry, i.e., spectrometers were symmetrically positioned with respect to the incident beam and a selection was made of secondary particles of the same momentum lying in a single scattering plane. It is obvious that the scattering angle of the nucleus is then fixed, and this severely limits the prospects of studying the knock-out reaction mechanism itself.

The study of (p, 2p) reactions has been pursued by several groups: in Chicago (460 MeV) [73], in Uppsala (185 MeV) [74], in Orsay (155 MeV) [75], in Liverpool (385 MeV) [38], etc. The resolution in the excitation energy of the residual nucleus in these experiments was about 3 MeV. A resolution of 1 MeV at an initial energy of 1 GeV was obtained in an investigation [76] of (p, 2p) reactions on C^{12} and D. The results of the experimental studies have usually been the spectra of excitation energies of the residual nuclei and the distributions in the angle between the outgoing protons for various ranges of excitation energy. Typical results are shown in Fig. 9, taken from [73]. In Fig. 9a we show the excitation spectrum of the B^8 nucleus from the reaction $Be^9(p, 2p)B^8$. Transitions to the ground state and to two excited levels (with excitation energies 9 and 16 MeV) are distinguished. The angular distribution of Fig. 9b, with a characteristic central minimum, indicates the knock-out of p-wave protons (more precisely, protons with orbital angular momentum $l \geq 1$); the distributions of Fig. 9c, having maxima in the vicinity of the peak for elastic pp scattering, are typical s-wave distributions.

Similar results have been obtained in studying reactions of the types (p, pd), (p, pα) and (α, 2α) [1,77,78]. In addition, a number of investigations have been made of (e, ep) reactions [39,79,80]. The greatest interest in these cases lies in the spectra of excitation energies of the residual nuclei. An example of such a spectrum for the reaction $Ca^{40}(e, ep)$ is shown in Fig. 10. The authors in-

terpret the irregularities in the behavior of the curve as a superposition of several maxima associated with transitions to excited levels of the residual nucleus, and they then draw the conclusion that there is a broad level with an excitation energy 50–60 MeV. It is not at all obvious that such an interpretation is justified. The need for a reliable identification of the reaction mechanism becomes particularly acute in this situation. This applies also to the conclusions that there exist highly excited states, which were reached on the basis of an analysis of (p, 2p) reactions on many nuclei at 385 MeV [38].

We could proceed with the discussion of spectroscopic information obtained in using high-energy particles to study nuclei. We shall confine ourselves to a reference to a detailed data compilation [81]. We stress once more that all these data are obtained under the assumption that the reactions have a quasi-elastic character. The criteria for the applicability of this approximation have not been tested. As we shall see below, it has not been possible to test the most sensitive criteria because the experiments have been staged with the symmetric coplanar geometry. To establish the reaction mechanism, we require "complete" experiments, and we now turn to the discussion of the latter.

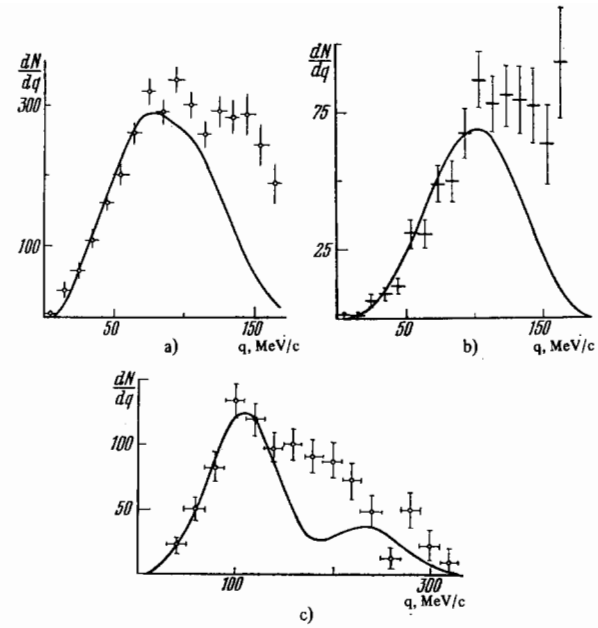

FIG. 11. The number of events of the (π^-, π^-p) reaction as a function of the momentum transferred to the residual nucleus for the reaction on Li^6 (a), Al^{27} (b) and C^{12} (c).

3. "Complete" experiments

By "complete" experiments, we mean here those experiments in which one measures the cross section as a function of all the independent kinematic variables (excluding the spin variables). In these experiments, at least one of the secondary fast particles is detected within a sufficiently large solid angle. For practical purposes, however, it is important to stress that in specific experimental conditions it is quite unnecessary for this angle to be 4π or thereabouts. To obtain information within the entire range of variation of, say, the Treiman-Yang angle, it is quite sufficient to detect the knock-out particle within a solid angle of the order of a radian. This is so because the events of greatest interest are those involving moderate momentum transfers, where most of the quasi-free scattering events are concentrated.

The first "complete" experiments which made it possible to test the majority of the criteria for the applicability of the pole approximation listed in Chap. II were begun in 1968 and are being successfully pursued at the Institute of Theoretical and Experimental Physics [17]. The (π^-, π^-p) reaction mechanism was studied at an initial pion momentum of about 1 GeV/c on the nuclei D, Li^6, C^{12} and Al^{27} [83-86]. The scattering angle of the secondary pion, whose momentum was measured by a magnetic spectrometer, was in the range 18–22°. The scattered protons were detected in a spark chamber placed near the target and subtending an angle of ±20°. The protons were stopped in the chamber, and their energy was measured according to their range. The experimental arrangement gave a poor resolution (~20 MeV) of the excitation energy of the residual nucleus and did not make it possible to obtain data referring to the individual levels. This was the chief shortcoming of these experiments, although it did not prevent definite conclusions from being drawn about the reaction mechanism.

In Fig. 11 we show typical distributions of the number of reaction events for a given momentum transfer q. This figure also shows the theoretical curves calculated in the pole approximation. We see that these curves provide a good description of the experimental data for small q, but deviate significantly from them for large momentum transfers. The theoretical curves are normalized so as to give the best fit in the small-q region; the normalization coefficient determines the reduced width of the transition $A \to B + p$. It should be remembered that there is another free parameter–the channel radius, which characterizes the form factor of the vertex. If the final-state level is not the only one, several parameters appear. In this case, allowance must be made for several form factors, generally with different l. Whenever this was a possibility, data from (p, 2p) reactions at lower energies were used for the channel radii and relative transition probabilities. Of course, as long as we consider only the distributions in the momentum of the residual nucleus, we may also achieve a better fit of the theory to the experimental data at large q by varying the shape of the form factor and the values of the reduced widths. However, the constants which characterize the $A \to B + p$ vertices will then themselves begin to depend on the range of q, the incident energy, the type of reaction and the nature of the incident particles. Such an ambiguity is inherent in one way or another in all known experimental data. It is clearly insufficient to consider only the distributions in q. Let us examine the other distributions that are obtained–and this is important–under identical conditions in a single experiment.

Figure 12 shows a typical form of the number of events of the (π^-, π^-p) reaction as a function of the Treiman-Yang angle, in various ranges of the momentum transfer q, for the case of the Li^6 nucleus. We see clearly that the isotropic distribution that is characteristic of the pole diagram is compatible with the experimental data only for small $q \sim q_0 = \sqrt{2m\epsilon}$, i.e., in the region in which the pole diagram gave a satisfactory description of the distribution in q. It is known that the pole diagram does not describe the entire process at larger q. This conclusion does not depend on the choice

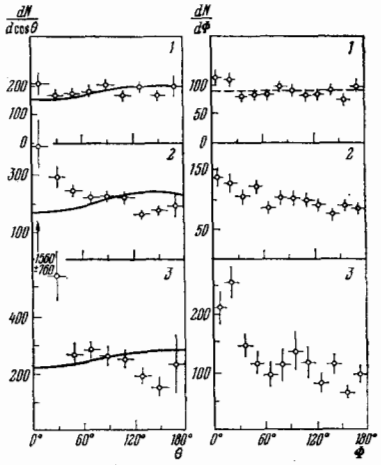

a) b)

FIG. 12. The number of events of the (π^-, π^-p) reaction on Li^6 as a function of the polar angle θ of the residual nucleus (a) and the Treiman-Yang angle (b) for the following ranges of momentum transfers: $0 < q < 80$ (1), $80 < q < 120$ (2) and $q > 120$ (3) MeV/c.

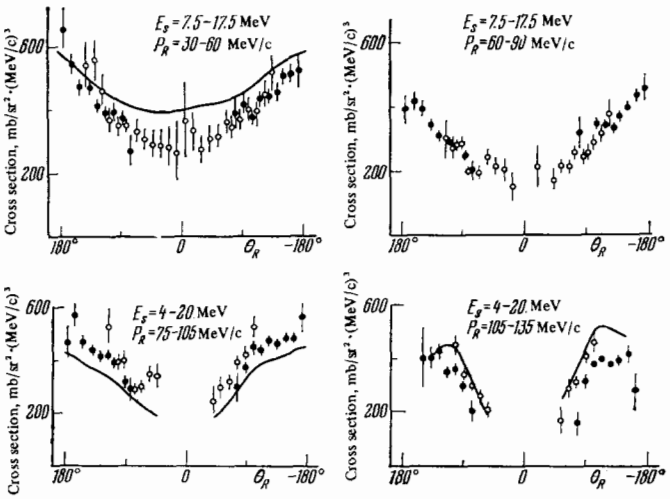

FIG. 13. The differential cross sections ofr the reaction Si^{28} (p, 2p) Al^{27*} as a function of the polar angle of the residual nucleus, for four ranges of the excitation energy of the nucleus and the momentum transferred to it [87].

of the form factor or on any model-dependent ideas. It is well confirmed by the distribution of recoil nuclei in the polar angle. Figure 12a shows the angular distributions of recoil nuclei for Li^6, together with the theoretical curves calculated in the pole approximation, for three ranges of q; we also show the data on the distributions in the Treiman-Yang angle (Fig. 12b). Similar results are obtained for other nuclei (C^{12}, Al^{27}).

In Fig. 13 we show the distribution in the polar angle of the residual nuclei for another class of reactions, namely the (p, 2p) reactions studied at an initial energy of 600 MeV in [87]. We have taken the reaction Si^{28}(p, 2p)Al^{27*} as an example. The four graphs in Fig. 13 correspond to different ranges of the excitation energy of the residual nucleus and the momentum transferred to it. To be sure, we are considering in all cases relatively small momentum transfers. The curves show the theoretical results, which represent in practice the calculation according to the pole diagram (although allowance is made for distorted waves, the distortions are small). The shape of the curves is determined to a great extent

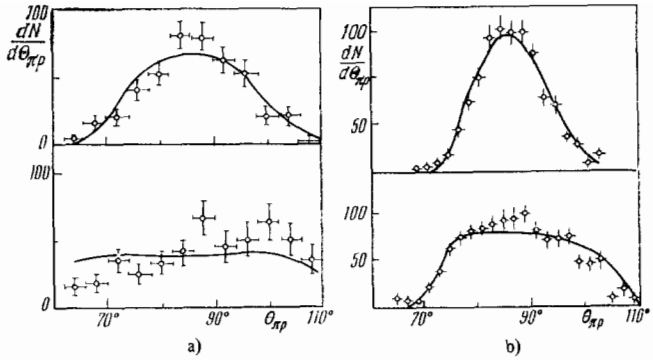

a) b)

FIG. 14. The distributions of the number of events of the (π^-, π^-p) reaction on the nuclei C^{12} (a) and Li^6 (b) as a function of the angle between the pion and proton. The upper curves are for momentum transfers $q < q_0$, and the lower curves are for $q > q_0$.

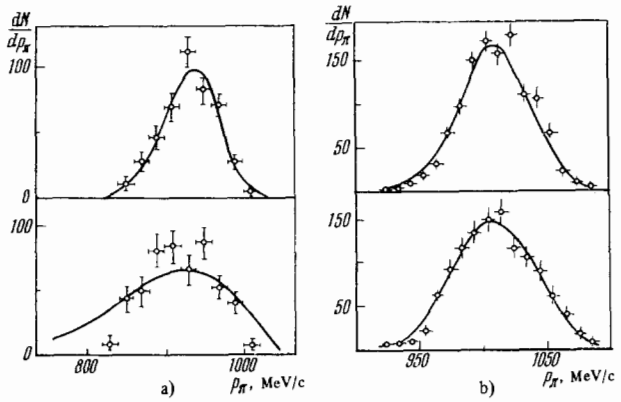

a) b)

FIG. 15. The spectra of pions emitted by the nuclei C^{12} (a) and Li^6 (b). The upper curves are for momentum transfers $q < q_0$, and the lower curves are for $q > q_0$.

by the efficiency of the experimental arrangement used in [87]. The normalization of the curves can, of course, also be varied in this case. It is clear from these and other data of this work that the curves provide a good description of the experimental results. The CERN work [87] was carried out with a "coplanar" geometry, which did not make it possible to obtain the distributions in the Treiman-Yang angle.

So far, we have discussed the distributions which are characteristic of the nuclear vertex in the pole diagram. It is instructive to look at the experimental data obtained under the same conditions, but referring to the vertex at which virtual scattering takes place. In Fig. 14 we see the distributions in the angles at which the pion and proton emerge from C^{12} and Li^6 nuclei in $(\pi, \pi p)$ reactions. Figure 15 shows the spectra of pions from the same nuclei at fixed angle. Both sets of data, taken from the ITEP work, are shown for various ranges of the momentum transfer. The distributions are different, but their comparison with the theoretical curves (the solid curves in the figures correspond to the pole diagram) indicates that the experimental points are satisfactorily described by the pole model in both of the ranges of momentum transfer $q < q_0$ and $q > q_0$. Further examples can be given. This shows that the various criteria have different sensitivities to the reaction mechanism and that the most crucial distributions are those in the Treiman-Yang angle and in the polar angle of the residual nuclei.

Those distributions (the spectrum of secondary particles at fixed angle) whose form was regarded as a dem-

onstration of the quasi-elastic character of the reaction in the early ("single-track") experiments turn out to be insensitive to the mechanism. To permit a comparison with experiments carried out using the old technique, the work on the (π^-, π^-p) reaction on Li^6 which we cited above [84] also gave the spectrum of pions emerging at a definite angle for the case in which we are not interested in the remaining particles, i.e., when neither the value of q nor even the reaction channel is fixed. The curve calculated according to the pole diagram provides a good description of the spectrum. And this is so despite the fact that, as is known from the detailed analysis of the reaction $Li^6(\pi^-, \pi^-p)$, only 40% of the events at the maximum are related to the pole mechanism! This figure is obtained as the ratio of the effective number of protons $N_{eff} = 0.6$ $(0 < q < 170$ MeV/c) determined from a correct analysis of the data to the number ($N_{eff} = 1.5 \pm 0.2$) determined from the area under the spectrum in the region $p_\pi > 950$ MeV/c. The ratio of the two values of Neff shows, incidentally, what a large error one may commit in extracting spectroscopic information from the results of single-track experiments.

It would seem very important to carry out a test of the mechanism which is based on a comparison of the absolute values of cross sections. To be specific, it would be convenient to make such a test by comparing the reduced widths referring to a particular nuclear vertex but determined in different experiments, in different reactions and at different energies. Unfortunately, such a program cannot be fully realized at the present time. The trouble is that a large portion of the data on direct reactions has been obtained under conditions in which it is impossible to distinguish either transitions to particular states of the final nucleus or the region of small momentum transfers. In other cases (including stripping and pick-up reactions and most of the (p, 2p) reactions that have been studied), no detailed investigation of the mechanism of the processes has been made, and it is not entirely certain that the pole mechanism dominates and that the corresponding reduced width is extracted correctly from the experimental data.

In spite of this, two important conclusions can be drawn. First, there are no known instances in which different data are clearly incompatible. Second, the values of θ^2 are in good mutual agreement in those cases in which a more or less correct comparison can be made. We shall quote the figures for the proton width of the C^{12} nucleus when the B^{11} nucleus is produced in its ground state [58]. The (p, 2p) reaction yields $\theta^2 = 0.78 \pm 0.10$ (460 MeV) and 0.35 ± 0.04 (155 MeV); from the data on the $(\pi, \pi N)$ excitation curve one obtains 0.55 ± 0.10, while from an analysis of the (π^-, π^-p) reaction in the region of small momentum transfers one finds 0.72 ± 0.15. The existing discrepancies between different values of the reduced proton widths of the Li^6 nucleus [84] were eliminated when allowance was made for the mechanism discussed at the end of the preceding section (see Fig. 5); this mechanism is important here because of the instability of the He^5 nucleus. For production of He^5 in the ground state, one finds for θ^2_p the value 0.39 ± 0.06 from the (p, 2p) data and 0.50 ± 0.20 from the (π^-, π^-p) data [61]. Nevertheless, to be sure, a true crucial comparison of the reduced widths, like the determination of the precise values themselves, is a matter for the future.

We have so far discussed experiments performed with the aid of electronics that has recently been connected to spark chambers. It might appear that bubble chambers and emulsions, with which measurements can always be made with a geometry close to 4π, are highly suitable for a "complete" experiment. However, the shortcomings of these techniques (the impossibility of selecting and analyzing a sufficient number of events of a given type, the difficulties of reliably identifying a reaction in photoemulsions, etc.) substantially reduce their effectiveness for a detailed study of the reaction mechanism. Nevertheless, some interesting data are obtained in these cases.

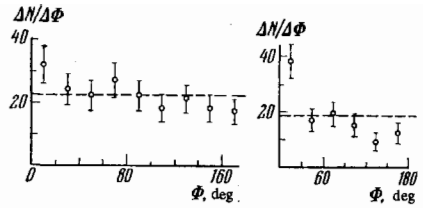

FIG. 16. The distribution of the number of events of the (π^+, π^+p) reaction in the Treiman-Yang angle, for two ranges of momentum transfers [88].

A specific study of the mechanism of nuclear reactions was carried out by the Leningrad group [88] in 1970 by means of nuclear photoemulsions. An investigation was made of (π^+, π^+p) and (π^+, π^0p) processes at an incident pion energy of 112 MeV. Unfortunately, the data refer to a mixture of light nuclei and the statistics are poor. However, certain perfectly concrete conclusions can be drawn. In Fig. 16 we give the most significant distribution in the Treiman-Yang angle, for two ranges of q that are comparable with those of the ITEP works [83-86]. It is readily seen that analogous results are obtained, on the basis of which the authors draw analogous conclusions. The same reactions of π^+ mesons in the carbon nucleus at 130 MeV were recently studied using a propane bubble chamber [89]. Finally, mention should be made of a study of the D(p, pn)p reaction carried out with a liquid hydrogen bubble chamber exposed to a beam of fast deuterons [90]. So far, only the traditional distributions have been published: proton momentum spectra and the number of reaction events as a function of momentum transfer. The results are in accord with those which are already available from experiments at other energies. However, we would like to point out the experimental technique itself. While enjoying the advantages of the chamber technique, it is free from one of its significant shortcomings, namely the impossibility of studying events involving small momentum transfers, since the slow recoil nucleon in the anti-laboratory system is a sufficiently fast particle in the laboratory system.

4. Estimate of the contribution of the pole mechanism

The data which we have considered enable us to say that, independently of the initial particle and its energy and the initial and final nuclear states, the pole mechanism gives the decisive contribution to the knock-out reaction in the region of small momenta $q < q_0$ transferred to the nucleus. Other diagrams provide a significant contribution at large momentum transfers.

In [84] it was attempted to give a quantitative estimate of the contribution of the pole diagram in relation to the contribution of the other diagrams over various ranges of q on the basis of the data on the (π^-, π^-p) reaction on the Li^6 nucleus, using a representation of the reaction amplitude in the form $M = M_{pole} + C$, where M_{pole} is the

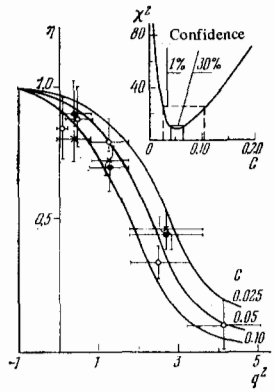

FIG. 17

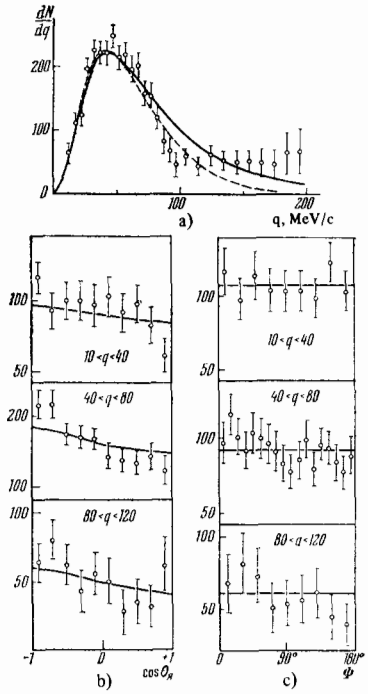

FIG. 18

FIG. 17. The ratio of the contribution of the pole diagram to that of all possible processes, as a function of the square of the momentum transfer in a reaction of the type $Li^6(\pi^-, \pi^-p)$.

FIG. 18. The number of events of the reaction $D(\pi^-, \pi^-p)$ as a function of the momentum transfer (a), the polar (b) and the azimuthal (c) scattering angle of the neutron. The various curves in b) and c) refer to different ranges of momentum transfer.

amplitude for the pole diagram and C is a q-independent quantity which has a phase $\pi/2$ with respect to M_{pole}. Therefore $|M|^2 = |M_{pole}|^2 + |C|^2$. It is assumed that the dependence of C on the other variables (including the spin variables) is such that the distributions in the Treiman-Yang angle and in the polar angle of the residual nucleus given by C do not contain a significant isotropic component. In that case, the anisotropic components of the distributions in the scattering angle of the nucleus and in the Treiman-Yang angle can be attributed entirely to non-pole mechanisms. The results are shown in Fig. 17. We have plotted here along the horizontal axis the value of q^2 in units of q_0^2, i.e., in units of the square of the distance to the pole, which lies at the point $q^2 = -1$. Along the vertical axis, we have plotted the ratio of the contribution of the pole diagram to that of all possible processes. Points indicated by different symbols have been obtained by analyzing different distributions; the light circles are from the distribution in q, the crosses are from the distribution in the Treiman-Yang angle, and the dark circles are from the distribution in the polar angle of the recoil nucleus. Since the various points must be regarded as independent, the fact that they are in agreement within the statistical errors is to some extent a justification of the assumptions made above. The solid curves in the figure are the theoretical results, which have the form of the ratio of the pole term to the sum of the pole term and a constant which makes crude allowance for the background. The value of the constant was varied. The inset to the figure shows χ^2 as a function of the value of the constant. The optimum value is $0.05^{+0.02}_{-0.01}$. The corresponding curve provides a good description of the experimental points and of course attains the value 1 at the pole.

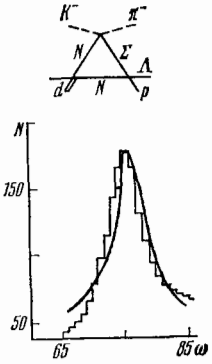

FIG. 19. The mass spectrum of the Λp system from the reaction $K^-d \to \pi^-\Lambda p$ [93]. The Λp kinetic energy is plotted along the horizontal axis.

Figure 17 enables us to draw the following conclusions. First of all, the pole contribution amounts to 80–90% for small $q < 1$, which allows us to say that the pole diagram gives the decisive contribution in this region. The contribution of the pole diagram falls off rapidly with q^2 (it is a curious fact that its fall-off is more rapid than for the $(\pi, 2\pi)$ reaction on the nucleon).

The rate of fall-off of the curve in Fig. 17 depends on the positions of the singularities which are nearest to the pole. In the case of the deuteron, for which the pole is anomalously close ($q_0 = 45$ MeV/c), we may expect a compression of the region in which the pole diagram dominates. Such a compression is actually observed up to $q \sim 120$ MeV/c, as can be seen, for example, from the experimental data on the reaction $D(\pi^-, \pi^-p)n$ near 1 GeV/c [85]. This follows from the distributions in the polar and azimuthal scattering angles of the recoil nucleus for the various q shown in Fig. 18. We see that, within the statistical accuracy, the pole curves describe the experimental points in all of the ranges of q that were studied. To be sure, the deviations from the pole curves become appreciable for still larger q [91].

IV. THE TRIANGLE MECHANISM

Let us turn to the discussion of some specific reactions for whose successful description it is important to allow for the triangle mechanism: $K^-d \to \pi^-\Lambda p$, the $(p, d\pi^+)$ reaction on light nuclei, and large-angle elastic pd scattering (an example of a binary process involving a large momentum transfer).

1. Mass spectrum of the Λp system in the reaction $K^-d \to \pi^-\Lambda p$

When one studies experimentally the mass spectrum of the Λp system produced in the capture of stopped K^- mesons by the deuteron (see, e.g., [92]), a pronounced maximum is observed near 2130 MeV, corresponding to the threshold for the reaction $\Lambda p \to \Sigma N$. One of the possible explanations is the assumption that there exists a resonance of mass 2130 MeV in the Λp system. However, as has been shown in [93], there is no need to introduce a new resonance to describe this peak, and one can explain it as a consequence of the threshold singularity of a diagram in which allowance is made for the interaction $\Sigma N \to \Lambda p$ in the final state (see the inset in Fig. 19). In a theoretical treatment, the amplitude for the reaction $K^-d \to \pi^-\Lambda p$ near the threshold for the reaction $\Lambda p \to \Sigma n$ was represented in the form

$$M(\omega) = M_\Delta(\omega) + C, \qquad (4.1)$$

where ω is the kinetic energy of the Λ and p in their c.m.s., $M_\Delta(\omega)$ is the amplitude corresponding to the

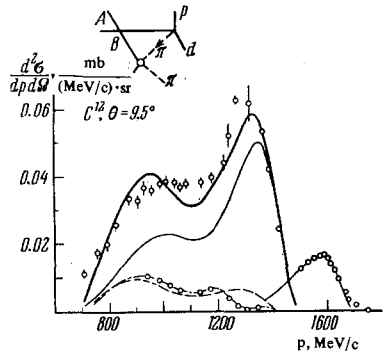

FIG. 20. The momentum spectrum of deuterons emitted at 9.5° from the C^{12} nucleus exposed to 670-MeV protons [70]. The thin solid curve takes into account only the pole diagram; the heavy solid curve also takes into account the triangle diagram shown in the inset; the dashed and dot-dash curves show the contributions of the triangle diagram and the interference term.

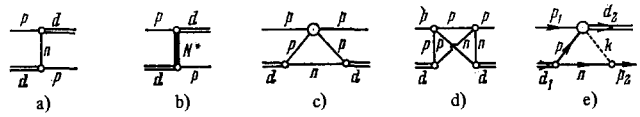

FIG. 21. Diagrams for elastic pd scattering.

diagram under consideration, and C is a complex constant which gives the contribution of all the other diagrams. The Hulthén form was employed for the deuteron wave function, the amplitude for the reaction $\Sigma N \to \Lambda p$ was assumed to be constant, and the amplitude for the reaction $K^- n \to \pi^- \Sigma$ was taken in the zero-range approximation. The real and imaginary parts of the constant C were adjustable parameters.

The results of the calculation are shown in Fig. 19. We also show there the experimental data. It can be seen that the theoretical curve is in good agreement with the experimental data. The spectrum from [92] shown in Fig. 19 is not normalized. Consequently, we cannot use these results to estimate the cross section for the reaction $\Sigma N \to \Lambda p$. However, if we make use of the data on the mass spectrum in a wider interval of the variable ω and assume that the entire "background" is produced by the pole diagram involving the vertex $K^- n \to \pi^- \Lambda$, we may conclude that the amplitude for the reaction $\Sigma N \to \Lambda p$ at threshold is of the same order of magnitude as the elastic Λp scattering length (~ -1.5 F).

Of course, none of the foregoing considerations rule out the possibility that there exists a resonance of mass 2130 MeV in the Λp system. To clarify the nature of the maximum in the mass spectrum, it would be necessary to study the reaction $K^- d \to \pi^- \Lambda p$ with fast kaons. If the maximum is really due to the singularities of the diagram in Fig. 19, then the shape and position of this maximum should vary with the momentum transferred from the kaon to the pion (see Chap. II).

2. Pion rescattering in the (p, dπ) reaction

In Chap. III we have already mentioned investigations of the spectra of fast deuterons produced in the interaction of 670-MeV protons with nuclei [70]. The main component of the spectrum is associated with the (p, dπ) reaction. A calculation based on the pole diagram involving the vertex $p + N \to d + \pi$ gives a good result for the high-momentum component of the spectrum, but leads to too low a value for the cross sections at lower momenta. The authors of [70] noted that rescattering of the produced pions by the residual nucleus may play a major role here. The point is that, when the scattering angle of the deuterons with respect to the proton beam is ~10°, the pions produced in the reaction $pp \to d\pi^+$ have an energy close to the resonant energy (~160 MeV) at which there is a maximum in the pion-nucleus interaction cross section. If allowance is made for the diagram shown in the inset to Fig. 20, the fit to the experimental data is greatly improved. In Fig. 20 we show the momentum spectrum of deuterons emerging at 9.5° from the C^{12} nucleus (the maximum at $p \approx 1600$ MeV/c is associated with the (p, pd) reaction). The dashed curve shows the theoretical result corresponding to the two pole diagrams for the (p, pd) and (p, dπ) reactions. The solid curve, which provides an excellent description of the experimental data, also includes the diagram of Fig. 20. This diagram turns out to be insufficient for heavier nuclei. In this case, more complex processes apparently play a major role.

3. Large-angle elastic pd scattering

Medium- and high-energy elastic pd scattering at angles near 180° is one of the simplest nuclear processes involving a large momentum transfer. There is no reliable theory of such processes at the present time. It may turn out that the main contribution here comes not from the mechanisms that have traditionally been considered in nuclear physics, but from more "exotic" ones such as those involving the virtual production of a pion or of nucleon isobars.

The experimental data [67b, 94] exhibit a sharp rise in the differential cross section towards 180° and an irregularity (an indication of a peak) in the energy dependence of the cross section at fixed angle in the energy range 600–700 MeV (this is the isobar, or resonance, region, since the $\Delta(1236)$ isobar can be produced here in the two-nucleon system).

The simplest mechanism that leads to a peak in the backward cross section is single-nucleon exchange (the diagram of Fig. 21a). However, while giving a satisfactory description of the experimental data in the low-energy region, the pole diagram of Fig. 21a already yields a cross section which is an order of magnitude below the experimental one at 1 GeV. Other possibilities have also been discussed in the literature: the exchange of one or of several nucleon isobars, beginning with the N (1688) [95] (Fig. 21b), the impulse approximation (Fig. 21c), and double scattering [96] (Fig. 21d). For a number of reasons, all of these models prove to be unsatisfactory (see [97] for further details). Moreover, they do not give a maximum in the energy dependence of the cross section at resonant energies. At the same time, owing to the large cross section for the reaction

$$p + p \to d + \pi^+ \qquad (4.2)$$

at these energies, the two-stage mechanism corresponding to the diagram of Fig. 21e turns out to be dominant: the incident proton interacts with one of the nucleons of the deuteron and the reaction (4.2) takes place, after which the pion which is produced is absorbed by the second nucleon. A pronounced resonance behavior of the cross section for the reaction (4.2) would lead to a corresponding peak in the pd scattering cross section. This mechanism for elastic pd scattering was proposed in [98] and studied in detail in [97] 18).

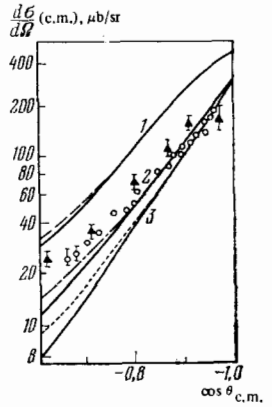

FIG. 22

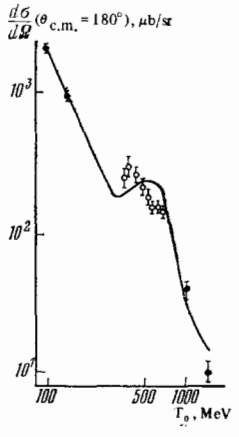

FIG. 23

FIG. 22. The angular distribution in elastic pd scattering at large angles for 600-MeV protons. Curve 1 is calculated with the Hulthén wave function, curve 2 with the Gaussian wave function, and curve 3 with the third function of Moravcsik [97].

FIG. 23. The energy dependence of the cross section for elastic pd scattering at 180° in the c.m.s. [97].

The angular distribution at 600 MeV, calculated in accordance with the diagram of Fig. 21e, is shown in Fig. 22 for various deuteron wave functions (Hulthén and Gaussian functions, and the third function of Moravcsik). It is readily seen that the result is strongly dependent on the choice of the wave function. Allowance for D-waves in the deuteron does not lead to significant modifications (see the dashed, dot-dash and dotted curves). In the same figure we show the experimental data, which are in qualitative agreement with the theory.

In calculating the energy dependence of the elastic pd scattering cross section, we added to the diagram of Fig. 22e a certain "background," which has a smooth energy dependence and corresponds to the contribution of the other diagrams (see Chap. II.3). As a model for the energy dependence of the background, we took the amplitude of the pole diagram of Fig. 22a, but with a certain factor determined by requiring the best fit to the experimental data. The results of such a fit at 180° are shown in Fig. 23. The background contributes about 4% to the cross section at the maximum. It is clear that the theoretical curve reflects more or less correctly the position and absolute value of the experimentally observed maximum in the energy dependence of the cross section. This fact favors the mechanism in question.

The study of polarization effects would open up a further possibility of elucidating the role of the diagram of Fig. 21e in the isobar region. The polarizations of the outgoing particles and the asymmetry in a reaction involving polarized incident particles can be expressed in terms of the analogous quantities for the process (4.2) or its inverse process [97]. Unfortunately, there are as yet no good data on the polarization and asymmetry in large-angle pd scattering, and it does not appear to be possible to test these predictions of the theory.

The mechanism under consideration apparently plays a major role not only in elastic pd scattering, but also in a number of other nuclear processes involving large momentum transfers, in particular in photonuclear (γ, p) reactions [101], where it affords an explanation of certain effects that are unexpected at first sight, and in the reaction $\pi^- d \to N\Delta$, which has recently been studied theoretically [102].

V. PION AND KAON CAPTURE

The energy spectra and angular correlations of the particles produced by the absorption of slow π^- and K^- mesons indicate that we are dealing with a direct process in an appreciable fraction of the events. In accordance with the subject of the present paper, we shall examine only the possible mechanisms of the capture. Other aspects of the physics of such processes are treated in the reviews [5, 103-106].

Single-nucleon capture of a slow pion is improbable, since, owing to the laws of conservation of energy and momentum (the nucleus contains a large energy and zero momentum), it can take place only on a nucleon which moves inside the nucleus with a momentum ~500 MeV/c. Since there are very few nucleons inside the nucleus with such a high momentum, a group of nucleons must take part in the absorption of pions. The fundamental problem is the following: does the capture of a meson occur on a virtual deuteron, α particle or other correlated group of nucleons that is virtually emitted by the nucleus (in this case, the reaction is described by the corresponding pole diagram or by the simplest diagrams which allow for the interaction of the secondary particles), or does a dynamical correlation of the nucleons occur in the capture process? The second alternative would imply that the correlation occurs during the direct capture process itself and is not "prepared" beforehand in the nucleus. Consider, for example, the reaction of producing a pion in a collision of two free (not nuclear) nucleons, $N+N \to N+N+\pi$. The amplitude for this reaction is a function of the kinematic variables, in particular the momentum transfers. This means that the particles will be correlated in a definite way, and this correlation will obviously depend on the reaction mechanism. Capture of a pion by a nucleon pair, $\pi+N+N \to N+N$, is the inverse reaction of the production process and is described by the same amplitude (with reversed signs of the momenta and spin projections). The correlations that are observed in the capture may be determined not so much by the nuclear wave function as by the amplitude for the free-particle process itself.

The greatest number of testable consequences can be obtained for the first of the above-mentioned mechanisms (the relative probabilities of the various channels, the energy and angular distributions of the products, and the dependence of the cross section on the energy of the absorbed pion). In this case, it is important to consider not only possible capture by a virtual deuteron, but also by other particles – α, t, etc. (there are no grounds for assigning a prior preference to any one of the enumerated virtual particles; moreover, for different nuclei and under different kinematic conditions, the main contribution may come from absorption by different virtual particles). It is well known that the two-nucleon capture mechanism [107], the simplest variant of which corresponds to the graphs a and b of Fig. 24, gives an appreciable contribution, at least in the region of small momenta transferred to the residual nucleus. For (π^-, nn) reactions, this region corresponds to a scattering angle between the two neutrons close to 180°. The experimental study of the reaction $Li^6(\pi^-, nn)$ shows conclusively that the neutrons are correlated in such a way that the angle between them is approximately

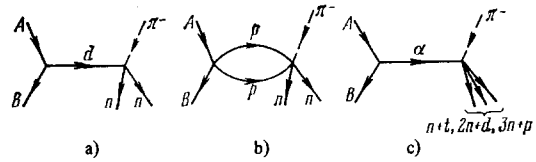

FIG. 24. Diagrams corresponding to π^--meson capture.

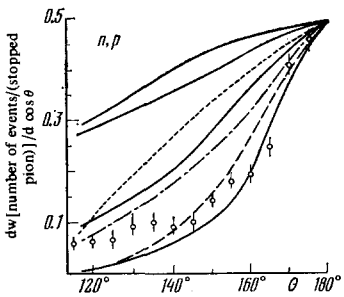

FIG. 25

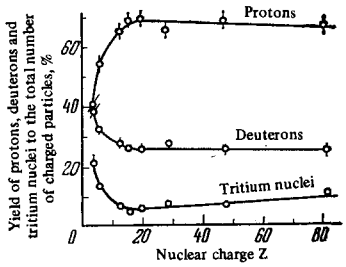

FIG. 26

FIG. 25. The distribution in the angle between the neutron and proton from the reaction $C^{12}(\pi^-, np)B^{10}$ [109]. The upper curve is the calculation according to the α-particle model, and the other curves are the calculations according to different variants of two-particle capture.

FIG. 26. The relative yields of protons, deuterons and tritium nuclei above 24 MeV [114].

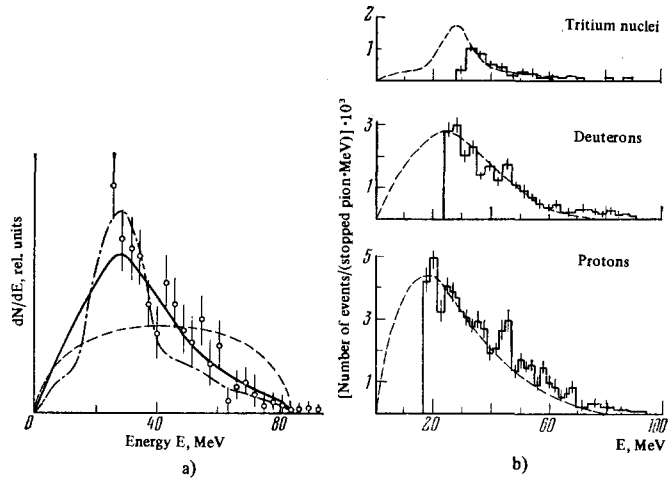

FIG. 27. Spectra of fast particles produced in capture by carbon. a) The spectrum of tritium nuclei from [114], b) spectra of protons, deuterons and tritium nuclei detected in coincidence with neutrons [109,117].

180° [108]. An equally sharp maximum in the angular dependence is observed in the reaction $C^{12}(\pi^-, np)B^{10}$ [109], as can be seen from Fig. 25. The curves are the results of the theoretical calculations. The group of lower curves shows the calculated results according to different variants of the model for two-nucleon absorption. The upper curve corresponds to α-particle capture, which leads to an angular correlation, but not such a sharp one. The experimental picture can be attributed to either capture by the deuteron, followed by charge exchange of one of the neutrons, or capture by a biproton pair. A sharp correlation also occurs in the second case [110].

Until recently, there had been no observations of the peak in the nucleon spectrum at ~(50–60) MeV which should occur if the capture takes place on two nucleons [111]. However, it was shown in a recent work [109] that this peak is seen if one considers only those events in the reaction $C^{12}(\pi^-, np)B^{10}$ which correspond to production of the ground state of the B^{10} nucleus.

In addition, there may also be a large contribution from a multi-nucleon capture mechanism such as the α-particle mechanism (Fig. 24c) [19]. The large quantity of data accumulated in works using bubble chambers and photoemulsions (see, e.g., [112], where references to the earlier investigations can be found) have not been able to provide information on multi-nucleon capture, since no distinction was made in these data between protons, deuterons and tritium nuclei. Such a distinction was first made in [113], where it was discovered that many deuterons and tritium nuclei are produced when slow pions are absorbed by the light nuclei of a photoemulsion. Figure 26 shows the relative yields of p, d and t that were recently measured with the electronics of [114]. For light nuclei in the region of carbon, the relative yields of hydrogen isotopes are approximately the same as for capture by He^4. The p, d and t spectra obtained in [113] are in agreement with the α-particle model [111].

The α-particle model of capture was proposed theoretically in [115] and analyzed in detail in [110,111,116]. It was shown [110] that a qualitative explanation can be given of all the comparatively crude experimental data on the angular correlations, spectra and absolute capture probabilities if allowance is made for both the two-nucleon mechanism and the α-particle mechanism. More detailed experiments, permitting a quantitative comparison with the α-particle model, were begun comparatively recently [114,117]. In Fig. 27a we show the spectrum of tritium nuclei produced in π^- capture by carbon [114]. The theoretical curves are from [111], and the dashed curve shows the phase space. The solid curve and the dot-dash curve are calculated according to the diagram of Fig. 24c without and with allowance for a nuclear form factor. We see that these two curves are in good agreement with the experimental data. The deuteron spectrum obtained in [114] is also in good agreement with the model of α-particle capture.

Figure 27b gives the spectra of protons, deuterons and tritium nuclei obtained in another work [117]. Charged particles were detected in coincidence with neutrons in capture by carbon. The dashed curves are calculated according to the α-particle model [111]. Figure 28 shows the angular correlations of (n, t) and (n, d) pairs obtained in [117]. The theoretical curves, taken from [116], are again calculated according to the α-particle model. The nature of the (n, d) correlation indicates a contribution from the diagram involving He^3 exchange. The same experiment gave the excitation spectrum of the residual nuclei from the reactions $C^{12}(\pi^-, nt)$, $C^{12}(\pi^-, nd)$ and $C^{12}(\pi^-, np)$, for events with a scattering angle between 170 and 180°. While a clear maximum is seen in the spectrum of nuclei from the first reaction, corresponding to production of the Be^8 nucleus in its ground state, no such maximum occurs in the spectra of nuclei from the second and third reactions. This again indicates that multi-nucleon capture plays a major role. It is well known, for example, that the α-particle mechanism simulates a broad excitation spectrum if nucleon pairs are detected [118].

Mention should be made of one more experiment, in which a photoemulsion technique was used to investigate the spectra of secondary particles and the angular correlations in the reaction $\pi^- + C^{12} \rightarrow Li^8 + He^3 + n$ [119]. It was found that these characteristics are in good agreement with the model of absorption by Li^4. Here, how-

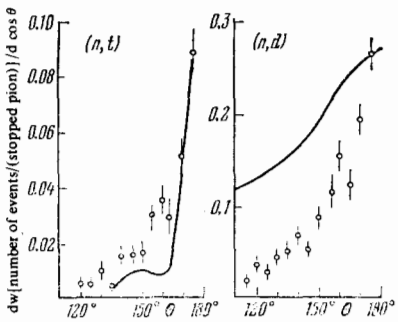

FIG. 28. The distribution in the angle between the pairs (n, t) and (n, d) after π^- capture by carbon [117].

ever, one requires a further test of whether these distributions can be the result of secondary processes which follow capture by a deuteron or α particle. The point is that the channel Li^8He^3n is rare (its relative probability is 2.2×10^{-4}), and various secondary processes, even if they are improbable, may give an appreciable contribution.

Thus, the existing experimental data indicate that multi-nucleon capture plays an important role. Nevertheless, a number of important questions remain unanswered. The possible role of rescattering of the particles after the process of pion capture (and, in general, the role of secondary processes) has so far been poorly studied theoretically. To study the α-particle capture mechanism experimentally, it would be especially valuable to make a more detailed study of the (π^-, tn) reaction in the region of small momenta of the residual nucleus, as well as the (π^+, He^3p) reaction at low energies. For the capture of pions in flight, there is an additional opportunity of testing the mechanism—the utilization of the Treiman-Yang criterion. Desirable experiments are discussed in greater detail in [14]. In investigations carried out with a high accuracy, it would naturally be necessary to allow for the fact that the pions are captured from various mesoatomic orbits [120], and this affects the characteristics of the process.

The currently available information on K^--meson capture is much more limited. In this case, in contrast with π^--meson absorption, single-nucleon capture accompanied by pion emission is possible, corresponding to the reaction $K^- + A \to Y + \pi + B$ (where Y is a hyperon, and B is the residual nucleus). The energy spectra and angular correlations of the pions and hyperons produced in K^- absorption by He^4 nuclei [121], in a propane-freon mixture and in photoemulsions [105,122] are in qualitative agreement with the predictions of the simple impulse approximation (the pole diagram involving nucleon exchange). However, the above-mentioned characteristics have so far been measured with very poor accuracy. The theoretical calculations here are also unreliable, since they make no allowance for the effect of the nearby subthreshold Y (1405) and Y (1385) resonances in the KN system, which lead to an appreciable energy dependence of the KN interaction amplitudes [123]. Allowance for these resonances in the K^- capture process and the determination of the parameters of their interaction with nucleons or with the residual nucleus represent some of the most interesting problems of the physics of kaon-nuclear interactions.

The non-mesonic captures $K^- + A \to Y + N + B$ can take place only on a group of nucleons. The fraction of such captures is $(1.22\pm0.9)\%$ for deuterons [124] and $(16.5\pm2.6)\%$ for He^4 nuclei [121]. For light nuclei (C, N and O), the fraction of non-mesonic captures is close to the figure for He^4 and amounts to 17–20%. Measurements have also been made of the spectra of fast nucleons, the distributions of stars in the number of rays, and the probabilities of various non-mesonic channels in the capture by deuterons [124] and by nuclei [125]. The data on the energy spectra of particles produced in K^- capture by light nuclei are compatible with our ideas about the α-particle capture mechanism [106].

Interest in studying the interaction of slow kaons with nuclei is associated to a great extent with the question of the neutron periphery of heavy nuclei. The point is that K^--meson capture should be very sensitive to the abundance of neutrons at the periphery of the nucleus, since, as a consequence of the high probability of capture (single-nucleon capture is allowed), the K^- mesons are absorbed mainly at the surface of the nucleus. It is also significant that different channels are realized for capture by neutrons and by protons (capture by neutrons proceeds mainly according to the scheme $K^- + n \to \Sigma^- + \pi^0$, $\Sigma^0(\Lambda^0) + \pi^-$, while capture by protons proceeds according to the scheme $K^- + p \to \Sigma^\pm + \pi^\mp$, $\Sigma^0(\Lambda^0) + \pi^0$). It is inferred from the data on K^- capture by heavy nuclei that the radius of the neutron distribution is appreciably larger than that of the proton distribution, i.e., that the periphery of the nucleus consists mainly of neutrons [126] (see also [127]). This conclusion is based on the fact that the ratio of the probabilities of the channels realized in K^- capture by the neutron and by the proton is four times as large for heavy nuclei as the corresponding quantity for light nuclei. However, there exist here a number of unresolved problems of both an experimental and theoretical nature (there is no reliable information on the capture mechanism, and it is difficult to make proper allowance for the strange resonances).

The analysis of the data on the intensities of the transitions in kaonic atoms [128] also seemed to require the assumption of a neutron periphery. However, more precise calculations [129], allowing for distortion of the Coulomb wave function of the kaonic atom at small distances caused by the strong interaction, have shown that this conclusion is premature, and the existing data (see also [130]) are consistent with the assumption that the proton and neutron distributions have the same radius. The results of a recent investigation of the interaction cross sections of positive and negative pions of momentum 0.71 to 2.0 GeV/c with lead nuclei [131] give evidence against the neutron periphery.

Thus, it is difficult to reconcile the available data with the assumption that there is a significant difference between the radii of the proton and neutron distributions. The question of a possible small difference remains open.

VI. CONCLUSIONS

In summary, it can be said that our theoretical ideas about the nature of direct processes at high energies are confirmed by the experimental data obtained in recent years. This means that the theoretically predicted dependences of the differential cross sections on the kinematic variables (the momentum transfer, scattering angles of the recoil nuclei, etc.) are observed experimentally. The experimental data also confirm the estimates of the domain of applicability of the theory, which

is confined to small momentum transfers to the nucleus. This shows that direct processes at high energies, by their physical nature, actually lead to an interaction of the incident particles with groups of nucleons that are virtually emitted by the nuclei.

The experimental data have shown, in particular, that the angular and momentum distributions that have been generally measured in the past are insensitive to the reaction mechanism and are therefore insufficient for a quantitative investigation of direct processes. The distributions which are most sensitive to the mechanism of the process are found to be those in the Treiman-Yang angle and the scattering angle of the recoil nucleus (with respect to the direction of the beam of incident particles). Recent results of the study of direct reactions induced by high-energy particles indicate that present-day experiments are capable of yielding the information required for the identification of the mechanism of a direct process.

At the present time, the firmest conclusions can be drawn about the mechanism of reactions of the quasi-elastic type. We note that, although such reactions have been studied for some time, it has been possible only very recently (and, moreover, in experiments with relativistic accelerators) to establish the domain of applicability of the pole mechanism corresponding to the picture of "simple knock-out" from the nucleus of nucleons, deuterons and other light nuclei ("clusters") by the incident particle. As was to be expected theoretically, simple knock-out occurs only when a rather small momentum is transferred to the residual nucleus, when, as a rule, no compression of the region of large momentum transfers is observed. In other words, quasi-elastic scattering takes place at the periphery of the nucleus. While this fact has been established quantitatively only for the knock-out of nucleons, it is worth emphasizing in this connection that there is no basis for the claims encountered in the literature that nuclei have a "cluster" structure, as if this has been demonstrated by experiments on direct reactions involving the knock-out of light nuclei. It is more likely that "clusters" are found with a certain probability only at the periphery of the nucleus.

When the program of theoretically desirable experiments formulated in the present review is compared with the experiments that have already been carried out, it can be seen that the study of direct reaction mechanisms more complex than the pole mechanism is still at its earliest stages. Next comes the informative experiments on the identification of some more complex mechanisms, in particular those corresponding to various triangle diagrams. It should be noted that practically no studies have been made so far of the relative roles of elastic and inelastic interaction processes in the "final" state of direct reactions.

We have already mentioned several times that investigations of direct nuclear reactions are of great interest for both the study of the nucleus and the determination of the properties of elementary particles. In this last case, we have had in mind mainly the extraction of information on the interaction of elementary particles from nuclear experiments. In conclusion, we would like to point out yet another, perhaps somewhat unexpected, aspect of the "collaboration" between nuclear physics and elementary particle physics. In recent years, it has been found that there is a certain similarity between the strong-interaction processes of elementary particles at high energies and nuclear processes. Briefly, a number of phenomena that accompany the collision of two particles with very high energies (of the order of 10 GeV in the c.m.s.) look as if these particles, like nuclei, have internal degrees of freedom. This circumstance has been reflected in the well-known "parton" model of high-energy collisions (partons are certain virtual "constituents" of an elementary particle, which exchange energy and momentum on undergoing collisions). The basic ideas of the parton model are borrowed from nuclear physics and correspond to the picture of direct reactions (at present, in the most primitive variant). Thus, the study of the mechanism of nuclear reactions may prove to be a significant heuristic aid in elucidating the physical nature of the interaction processes of elementary particles at high energies (the interrelationship of these two fields is also facilitated at the present time by a common theoretical language).

APPENDIX I

The amplitude M' for the reaction $i+x \to y+z$ can be expressed in the following way [12,20,23] in terms of the invariant amplitudes f, which depend only on the kinematic invariants characterizing this reaction:

$$(M')^{\mu_z\mu_y}_{\mu_i\mu_x} = \sum_{j_{ix}j_{zy}L\lambda} f(j_{ix}j_{zy}L\lambda)\, C^{j_{ix}\mu_{ix}}_{j_i\mu_i j_x\mu_x} C^{j_{zy}\mu_{zy}}_{j_z\mu_z j_y\mu_y} \times C^{j_{zy}\mu_{zy}}_{j_{ix}\mu_{ix}LM} C^{LM}_{r-\lambda,\, m_{ix},\, r+\lambda,\, m_{zy}} Y^*_{r-\lambda,\, m_{ix}}(\mathbf{n}_{ix})\, Y^*_{r+\lambda,\, m_{zy}}(\mathbf{n}_{zy}). \tag{A.1}$$

If the product of the intrinsic parities of the initial and final particles is equal to 1, then

$$r = \begin{cases} L/2, & \text{if } L \text{ is even,} \\ (L+1)/2, & \text{if } L \text{ is odd.} \end{cases}$$

If this product is equal to -1, then

$$r = \begin{cases} (L+1)/2, & \text{if } L \text{ is even,} \\ L/2, & \text{if } L \text{ is odd.} \end{cases}$$

The quantity λ runs over all integral (if r is integral) or half-integral (of r is half-integral) values for which the triplet $r-\lambda$, $r+\lambda$, L forms a triangle. n_{ix} and n_{zy} are unit vectors along the relative velocities of particles i and x and particles z and y. j_{ix} and j_{zy} are the spins of the incoming and outgoing channels, and L is their vector difference.

This representation is not unique. We could have written an expression for M' by introducing the total spins of the crossed channel, etc. A more detailed account of pertinent material can be found in [12,20].

By making use of Eqs. (2.6) and (A.1) and a graphical method of representing the sum of Clebsch-Gordan coefficients [12,24], we obtain for the quantity $\overline{|M|^2}$, Eq. (2.9), the following schematic representation [20]:

$$\overline{|M|^2} \sim \sum \gamma_{lJ}\gamma^*_{l'J'} F_{lJ}(q)\, F^*_{l'J'}(q)\, f(j_{ix}j_{zy}L\lambda) \times f^*(j'_{ix}j'_{zy}L'\lambda')\,(2a+1)(2b+1)(2c+1)\,\Phi_{abc}(\mathbf{n}_{ix}, \mathbf{n}_{zy}, \mathbf{n}_{iB}) \tag{A.2}$$

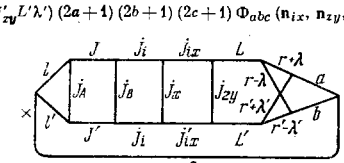

The summation runs over J, J', l, l', j_{ix}, j_{zy}, j'_{ix}, j'_{zy}, L, λ, L', λ', a, b and c, and Φ_{abc} are rotationally invariant combinations of the vectors n_{ix}, n_{zy}, and n_{iB}:

$$\Phi_{abc}(\mathbf{n}_{ix}, \mathbf{n}_{zy}, \mathbf{n}_{iB}) = \sum_{m_a m_b m_c} \begin{pmatrix} a & b & c \\ m_a & m_b & m_c \end{pmatrix} Y_{am_a}(\mathbf{n}_{ix})\, Y_{bm_b}(\mathbf{n}_{zy})\, Y_{cm_c}(\mathbf{n}_{iB}). \quad (A.3)$$

Since l and l' have the same parity, c is necessarily even.

APPENDIX II

We shall write down a number of formulas expressing the distributions in the reaction A + x → B + y + z in terms of the total (σ_0) and differential ($d\sigma_0/d\Omega$) cross sections for the reaction i + x → y + z when the amplitude is described by the pole diagram of Fig. 1.

Let p_X be the momentum of the incident particle in the laboratory system, and q and z be the momentum and cosine of the polar angle of the nucleus B. Then, introducing the notation

$$\Phi(q) = \frac{|F(q)|^2}{(q^2 - \varkappa^2)^2}, \quad (A.4)$$

we have

$$\frac{d\sigma}{dz} = \int_0^{q_{max}} q^2 \Phi(q)\, \sigma_0(s_{yz})\, dq, \quad (A.5)$$

where syz is the square of the sum of the 4-momenta of particles y and z:

$$s_{yz} \approx (m_A + \varepsilon_x - m_B)^2 - \frac{q^2}{|m_B|}(m_A + \varepsilon_x) - p_x^2 + 2p_x q z, \qquad \varepsilon_x = \sqrt{m_x^2 + p_x^2}. \quad (A.6)$$

q_{max} is defined by the expression

$$q_{max} = Bz + \sqrt{B^2 z^2 + C}, \quad (A.7)$$

where

$$B = \frac{m_B p_X}{m_A + \varepsilon_x},$$

$$C = \frac{m_B}{m_A + \varepsilon_x}\{(m_A + \varepsilon_x - m_B - m_y - m_z)(m_A + \varepsilon_x - m_B + m_y + m_z) - p_x^2\}.$$

The distribution in the momentum of the residual nucleus can be expressed as

$$\frac{d\sigma}{dq} \sim q\Phi(q) \int_{s_{yz}^{min}}^{s_{yz}^{max}} \sigma_0(s_{yz})\, ds_{yz}, \qquad s_{yz}^{min} = \max\{s_{yz}^{(2)}, (m_y + m_z)^2\}, \quad s_{yz}^{max} = s_{yz}^{(1)}, \quad (A.8)$$

where, for $q^2 \ll 4m_B^2$,

$$s_{yz}^{(1,2)} \approx (m_A + m_x)^2 + m_B^2 + 2m_A\varepsilon_x - \frac{m_A + \varepsilon_x}{m_B}(q^2 + 2m_B^2) \pm 2p_x q.$$

The distribution in the invariant mass of the (y + z) system is given by

$$\frac{d\sigma}{ds_{yz}} \sim \sigma_0(s_{yz}) \int_{q_{min}}^{q_{max}} \Phi(q)\, q\, dq. \quad (A.9)$$

The limits of integration are determined by very simple considerations. There are, as it were, two final-state particles—the nucleus B and the system y + z of mass $\sqrt{s_{yz}}$; q_{min} and q_{max} are reached when the angle between the directions of the momenta of the nuclei A and B is equal to 0 and 180° in the c.m.s. Unfortunately, the explicit expression is rather cumbersome (see, e.g., [33]).

The last distribution which we shall consider is the momentum distribution of the particles z detected at a fixed angle. To calculate this distribution, it is convenient to go over to an integration over the solid angle 4π in the c.m.s. of particles B and y (the P-system), expressing q and the variables on which $\overline{|M'|^2}$ depends in terms of the variable angles θ^P and φ^P:

$$\frac{d^2\sigma}{dp_z\, d\Omega_z} \sim \frac{p_z^2}{\varepsilon_z} \frac{p}{\sqrt{s_{By}}} \int \Phi(q)\, \overline{|M'|^2}\, d\cos\theta^P d\varphi^P, \quad (A.10)$$

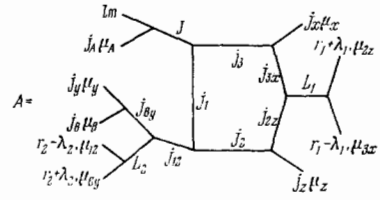

FIG. 29

where p is the momentum of particles B and y in the P-system.

APPENDIX III

Let us apply the graphical method of representing sums of Clebsch-Gordan coefficients [24] and present the graphical scheme for carrying out the summation over the spin projections of the virtual particles in Eq. (2.21) for the triangle diagram. We employ for the amplitudes M_1 and M_2 expansions of the type (A.1) involving the invariant amplitudes f_1 and f_2, and Eq. (2.6) for the amplitude Γ. We then obtain, accurate to within numerical coefficients (a sum over all the parameters except f_1, f_2 and f_3 is implied).

$$\Gamma^{\mu_1\mu_3}_{\mu_A}(M_1)^{\mu_2\mu_z}_{\mu_3\mu_x}(M_2)^{\mu_B\mu_y}_{\mu_1\mu_2} = \gamma_{1J} F_{1J}(q_{13})\, f_1(j_{3x} j_{2z} r_1 \lambda_1)\, f_2(j_{12} j_{By} r_2 \lambda_2)\, Y_{lm}(\mathbf{n}_{13}) \times Y^*_{r_1 - \lambda_1 \mu_{3x}}(\mathbf{n}_{3x})\, Y^*_{r_1 + \lambda_1 \mu_{2z}}(\mathbf{n}_{2z})\, Y^*_{r_2 - \lambda_2 \mu_{12}}(\mathbf{n}_{12}) \times Y^*_{r_2 + \lambda_2 \mu_{By}}(\mathbf{n}_{By})\, A(j_1, j_2, j_3, J, \ldots; m, \mu_A, \mu_x, \ldots),$$

where A denotes a quantity which, to within factors of the form $(2j_i + 1)$ and a sign, coincides with the 3jm coefficient represented by the diagram of Fig. 29.

---

[1] By the triangle mechanism we mean the set of three elementary interaction events corresponding to the triangle Feynman diagram.

[2] The general theoretical foundations of the method of nonrelativistic Feynman diagrams and its application to direct nuclear reactions are covered rather thoroughly in [7,8,17]. In what follows, we therefore confine ourselves to the study of some of the simple, but most important, diagrams. We shall also not consider the problems connected with the kinematics of a reaction, phase-space distributions, etc., as these problems are discussed in detail in [8,13,18].

[3] We shall adopt throughout this paper the system of units in which $\hbar = c = 1$.

[4] The reduced width θ^2 is often written in the form $\theta^2 = S\theta_0^2$, where S is a spectroscopic factor and θ_0^2 is the single-particle width (i.e., the width that we would have in a single-particle model) [22].

[5] Eq. (2.11) is written for the case in which only the reduced vertex part with definite values of l and J is non-zero. In the general case, there would appear a sum over these parameters.

[6] Problems connected with the fact that one of the particles taking part in the reaction i + x → y + z is virtual are considered in [8]. In some cases, its virtual nature can significantly alter the result (see, e.g., [26]).

[7] For sufficiently high energies in the cases of small q, if the particle z is fast, the Treiman-Yang angle coincides with good accuracy with the "azimuthal" angle, defined as the angle between the (p_X, p_B) and (p_X, p_Z) planes (all momenta are in the laboratory system) [29].

[8] Some caution is required here, however. For example, if we examine the distribution in the relative energy of particles y and z in the reaction (2.4) at a fixed initial energy, it will be concentrated near a certain value determined by the kinematics and by the fact that the pole mechanism distinguishes small q. In this case, a resonance in the reaction (2.4) will lead to a shrinkage or distortion of the peak in the distribution in s_{yz}. When analyzing different dependences of the cross section on the kinematic variables, one must also take into account the fact that the phase space is a rapidly varying function of these variables in many cases [8,13].

[9] We note that the numerical results of [42], in which the diagram involving rescattering of the isobar by the nucleus was considered for the reaction $C^{12}(\pi^-, \pi^-n)C^{11}$, are not quite correct. The corresponding mechanism does not lead to a maximum in the cross section in the energy region 120-150 MeV.

[10]Fortunately, exceptions sometimes occur, when one may establish definite isotopic relations [34], predict polarization effects (see Chap. IV.3), observe the dependence in the energy behavior of the cross section corresponding to the production of particles 1 and 2 with a large mass in the intermediate state, etc. However, such situations do not occur frequently and, in any case, are not the general rule, as was the case for the pole mechanism.

[11]The possibility of producing such systems has been investigated theoretically in [53].

[12]The point is that the corresponding integrals in the coordinate representation (see below) coverge rather rapidly, owing to the presence of a factor $\exp(-\kappa r)$ in the wave function. The integrals in the momentum representation are very slowly convergent.

[13]A similar method has been employed to analyze pd interactions [59].

[14]However, this does not mean that only elastic rescattering is taken into account. In fact, the correction term represents the sum of an infinite series of diagrams with a similar spin structure.

[15]The corresponding diagrams have a singularity in the momentum transferred from the initial nucleus to the final "nuclear system" which is closer than that of the pole diagram involving the vertex $Li^6 \to He^5 + p$.

[1]M. Riou, Rev. Mod. Phys. **37**, 330 (1965).

[2]G. Jacob and Th. A. Maris, ibid. **38**, 121 (1966); **45**, 6 (1973); T. Berggren and H. Tyren, Ann. Rev. Nucl. Sci. **16**, 153 (1966).

[3]a) C. Zupancic, in: High Energy Physics and Nuclear Structure (Proc. of the 2nd Intern. Conference), Amsterdam, North-Holland, 1967, p. 188; b) N. Tanner, in: High Energy Physics and Nuclear Structure (Proc. of the 3rd Intern. Conference), N.Y., Plenum Press, 1970, p. 346.

[4]V. I. Komarov, in: Trudy IV Mezhdunarodnoĭ konferentsii po fizike vysokikh énergiĭ i strukture yadra (Proc. of the 4th Intern. Conference on High-Energy Physics and Nuclear Structure), Dubna, JINR, 1972, p. 93.

[5]T. I. Kopaleĭshvili, Probl. fiz. ÉChAYa **2**, 439 (1971) [Sov. Phys. Part. Nuc. **2**, No. 2, 87 (1972)].

[6]D. S. Koltun, in: Advances in Nuclear Physics, Ed. M. Baranger and E. Vogt, Vol. 3, N.Y. and London, Plenum Press, 1969, p. 71.

[7]I. S. Shapiro, Teoriya pryamykh yadernykh reaktsiĭ (Theory of Direct Nuclear Reactions), Moscow, Atomizdat, 1963.

[8]I. S. Shapiro, Usp. Fiz. Nauk **92**, 549 (1967) [Sov. Phys.-Usp. **10**, 515 (1968)].

[9]I. S. Shapiro, in: Trudy problemnogo simpoziuma po fizike yadra (Proc. of the Problem Symposium on Nuclear Physics), Tbilisi, April 1967, Vol. 2, Moscow, ITEP, 1967, p. 307.

[10]G. A. Leksin, ibid., p. 321.

[11]V. M. Kolybasov and I. S. Shapiro, Identification of the Mechanism of Direct Processes Involving the Production of Three Particles. Review talk at the 18th Annual Meeting on Nuclear Spectroscopy and Structure of the Atomic Nucleus, Riga, 1968; ITEP Preprint No. 591, Moscow, 1968.

[12]V. M. Kolybasov, in: Materialy tret'eĭ zimneĭ shkoly po teorii yadra i fizike vysokikh énergiĭ (Proc. of the Third Winter School on Nuclear Theory and High-Energy Physics), Leningrad, LFTI, USSR Academy of Sciences, 1968, p. 211.

[13]V. M. Kolybasov, in: Materialy chetvertoĭ zimneĭ shkoly po teorii yadra i fizike vysokikh énergiĭ (Proc. of the Fourth Winter School on Nuclear Theory and High-Energy Physics), Part 1, Leningrad, LFTI, USSR Academy of Sciences, 1969, p. 34.

[14]V. M. Kolybasov and I. S. Shapiro, ITEP Preprint No. 785, Moscow, 1970.

[15]V. M. Kolybasov, in: Problemy sovremennoĭ yadernoĭ fiziki, Moscow, Nauka, 1971, p. 391.

[16]G. A. Leksin, in [4], p. 117.

[17]L. D. Blokhintsev, Diagrammatic Techniques in the Theory of Direct Nuclear Reactions (Lectures at the First Session of the All-Union School on Theoretical Nuclear Physics), Moscow, MIFI, 1971.

[18]V. M. Kolybasov, General Properties of the Scattering Matrix and Polarization Effects in Direct Nuclear Reactions (Lectures at the Second Session of the All-Union School on Theoretical Nuclear Physics), Moscow, MIFI, 1971.

[19]G. A. Leksin, Experimental Studies of the Mechanism of Nuclear Reactions at High Energies (Lectures at the Third Session of the All-Union School on Theoretical Nuclear Physics), Moscow, MIFI, 1972.

[20]I. S. Shapiro, V. M. Kolybasov and G. R. Augst, Nucl. Phys. **61**, 353 (1965).

[21]I. S. Shapiro and S. F. Timashev, Yad. Fiz. **2**, 445 (1965) [Sov. J. Nucl. Phys. **2**, 319 (1966)].

[22]M. H. Macfarlane and J. B. French, Rev. Mod. Phys. **32**, 567 (1960).

[23]S. M. Bilenky, L. I. Lapidus L. D. Pusikov and R. M. Ryndin, Nucl. Phys. 7, 646 (1958).

[24]A. P. Yutsis, I. B. Levinson and V. V. Vanagas, Matematicheskiĭ apparat teorii momenta kolichestva dvizheniya (Mathematical Techniques of Angular Momentum Theory), Vilnius, Gospolitnauchizdat, 1960.

[25]E. Ferrari and F. Selleri, Nuovo Cimento Suppl. **24**, 453 (1962).

[26]L. D. Blokhintsev and É. I. Dolinskiĭ, Yad. Fiz. 5, 115 (1967) [Sov. J. Nucl. Phys. **5**, 79 (1967)].

[27]V. M. Kolybasov, Yad. Fiz. **8**, 898 (1968) [Sov. J. Nucl. Phys. **8**, 522 (1969)].

[28]S. B. Treiman and C. N. Yang, Phys. Rev. Lett. **8**, 140 (1962).

[29]L. S. Vorob'ev, V. M. Kolybasov, V. L. Stolin and V. D. Khovanskiĭ, Yad. Fiz. **12**, 1218 (1970) [Sov. J. Nucl. Phys. **12**, 669 (1971)].

[30]H. R. Bleiden, Phys. Lett. 9, 176 (1964).

[31]I. S. Shapiro and V. M. Kolybasov, ZhETF Pis. Red. **4**, 329 (1966) [JETP Lett. 4, 221 (1966)].

[32]V. M. Kolybasov, Yad. Fiz. **5**, 288 (1967) [Sov. J. Nucl. Phys. **5**, 202 (1967)]; V. M. Kolybasov and N. Ya. Smorodinskaya, Yad. Fiz. **14**, 590 (1971) [Sov. J. Nucl. Phys. **14**, 330 (1972)].

[33]V. M. Kolybasov, Yad. Fiz. **2**, 144 (1965) [Sov. J. Nucl. Phys. **2**, 101 (1966)].

[34]V. M. Kolybasov and N. Ya. Smorodinskaya, Phys. Lett. **B30**, 11 (1969).

[35]I. S. Shapiro and V. M. Kolybasov, Nucl. Phys. **49**, 515 (1963).

[36]V. M. Kolybasov and I. S. Shapiro, Phys. Lett. **B25**, 497 (1967).

[37]V. M. Kolybasov and N. Ya. Smorodinskaya, Yad. Fiz. **15**, 483 (1972) [Sov. J. Nucl. Phys. **15**, 269 (1972)].

[38]A. N. James, P. T. Andrews et al., Nucl. Phys. **A133**; 89; **A138**, 145 (1969).

[39]U. Amaldi et al., Phys. Lett. **22**, 593 (1966); **B25**, 24 (1967); U. Amaldi, Preprint ISS 66/40 (1966).

[40]D. T. Chivers, E. M. Rimmer, B. W. Allerdyce et al., Nucl. Phys. **A126**, 129 (1969).

[41]P. L. Reeder and S. S. Markovitz, Phys. Rev. **B133**, 639 (1964).

[42]O. D. Dalkarov, Phys. Lett. **B26**, 610 (1968).

[43]J. Rohlin, S. Rohlin, B. W. Allardyce et al., Nucl. Phys. **B37**, 461 (1972).

[44]P. W. Hewson, ibid. **A133**, 659 (1969).

[45]L. D. Blokhintsev, É. I. Bolinskiĭ and V. S. Popov, Zh. Eksp. Teor. Fiz. 43, 2290 (1962) [Sov. Phys.-JETP

16, 1618 (1963)].
[46]B. N. Valuev, Zh. Eksp. Teor. Fiz. **47**, 649 (1964) [Sov. Phys.-JETP **20**, 433 (1965)]; V. V. Anisovich and L. G. Dakhno, Zh. Eksp. Teor. Fiz. **46**, 1152 (1964) [Sov. Phys.-JETP **19**, 779 (1964)].
[47]É. I. Dubovoĭ and I. S. Shapiro, Zh. Eksp. Teor. Fiz. **51**, 1251 (1966) [Sov. Phys.-JETP **24**, 839 (1967)]; **53**, 1395 (1967) [**26**, 809 (1968)].
[48]L. D. Blokhintsev, É. I. Dolinskiĭ and V. S. Popov, Zh. Eksp. Teor. Fiz. **42**, 1636 (1962) [Sov. Phys.-JETP 15, 1136 (1962)]; **43**, 1914 (1962) [16, 1350 (1963)].
[49]É. I. Dubovoĭ, ZhETF Pis. Red. 6, 777 (1966) [JETP Lett. 6, 240 (1967)].
[50]O. D. Dal'karov and I. S. Shapiro, Yad. Fiz. 7, 562 (1968) [Sov. J. Nucl. Phys. 7, 349 (1968)]; Phys. Lett. **B26**, 706 (1968).
[51]R. A. Lundy, I. A. Pless, D. R. Rust et al., Phys. Rev. Lett. **20**, 283 (1968).
[52]G. A. Leksin, in [12], p. 548; [15], p. 511.
[53]L. A. Kondratyuk and I. S. Shapiro, Yad. Fiz. **12**, 401 (1970) [Sov. J. Nucl. Phys. **12**, 220 (1971)]; V. A. Karmanov, L. A. Kondratyuk and I. S. Shapiro, ZhETF Pis. Red. **11**, 543 (1970) [JETP Lett. **11**, 374 (1970)]; V. A. Karmanov, L. A. Kondratyuk and I. S. Shapiro, Zh. Eksp. Teor. Fiz. **61**, 2185 (1971) [Sov. Phys.-JETP **34**, 1172 (1972)]; ZhETF Pis. Red. **14**, 127 (1971) [JETP Lett. **14**, 84 (1971)]; V. A. Karmanov, L. A. Kondratyuk and I. S. Shapiro, in [15], p. 496.
[54]O. D. Dal'karov and V. M. Kolybasov, Yad. Fiz. 18, 809 (1973).
[55]E. S. Abers, H. Burkhardt, V. L. Teplitz and C. Wilkin, Nuovo Cimento **42**, 365 (1966).
[56]L. D. Blokhintsev, É. I. Dolinskiĭ and V. V. Turovtsev, Vestn. Mosk. un., ser. "Fizika. Astronomiya", No. 1, 49 (1968).
[57]V. A. Kaminskiĭ, Yu. V. Orlov and I. S. Shapiro, Zh. Eksp. Teor. Fiz. **51**, 1236 (1966) [Sov. Phys.-JETP **24**, 829 (1967)].
[58]V. M. Kolybasov and N. Ya. Smorodinskaya, Nucl. Phys. **A136**, 165 (1969).
[59]V. V. Komarov and A. M. Popova, Nucl. Phys. **69**, 253 (1965); A. M. Popova and S. Muskalu, Yad. Fiz. **1**, 776 (1965) [Sov. J. Nucl. Phys. **1**, 555 (1965)].
[60]V. M. Kolybasov, Nucl. Phys. 68, 8 (1965).
[61]Yu. D. Bayukov, L. S. Vorob'ev, V. M. Kolybasov, G. A. Leksin, N. Ya. Smorodinskaya, V. L. Stolin and V. B. Fedorov, ZhETF Pis. Red. **17**, 629 (1973) [JETP Lett. **17**, 442 (1973)].
[62]O. Chamberlain and E. Segrè, Phys. Rev. **87**, 81 (1952).
[63]J. B. Cladis, W. N. Hess and B. J. Moyer, ibid., p. 87.
[64]L. S. Azhgireĭ et al., Zh. Eksp. Teor. Fiz. **36**, 1631 (1959) [Sov. Phys.-JETP **9**, 1163 (1959)].
[65]J. Steinberger and A. S. Bishop, Phys. Rev. **78**, 494 (1950).
[66]Yu. P. Antuf'ev et al., Yad. Fiz. **9**, 921 (1969) [Sov. J. Nucl. Phys. **9**, 538 (1969)]; **12**, 1143 (1970) [**12**, 627 (1971)]; **13**, 473 (1971) [**13**, 265 (1971)].
[67]a) L. S. Azhgireĭ et al., Zh. Eksp. Teor. Fiz. **33**, 1185 (1957) [Sov. Phys.-JETP **6**, 911 (1958)]; b) G. A. Leksin, ibid. **32**, 440 (1957) [5, 371 (1957)].
[68]D. I. Blokhintsev, Zh. Eksp. Teor. Fiz. 33, 1295 (1957) [Sov. Phys.-JETP 6, 995 (1958)].
[69]R. J. Sutter et al., Phys. Rev. Lett. **19**, 1189 (1967).
[70]L. S. Azhgireĭ et al., Yad. Fiz. **13**, 6 (1971) [Sov. J. Nucl. Phys. **13**, 3 (1971)]; L. S. Azhgireĭ et al., Nucl. Phys. **A195**, 581 (1972).
[71]V. I. Komarov, G. E. Komarov and O. V. Savchenko, Yad. Fiz. **11**, 711 (1970) [Sov. J. Nucl. Phys. **11**, 399 (1970)].
[72]H. Tyren et al., Nucl. Phys. 7, 10 (1958).
[73]G. Tibell, O. Sundberg and P. V. Renberg, Ark. Fys. **25**, 433 (1964).
[74]H. Tyren et al., Nucl. Phys. **79**, 321 (1966).
[75]M. Arditi et al., ibid. **A95**, 545; **A103**, 319 (1967).
[76]W. D. Simpson et al., Nucl. Phys. **A140**, 201 (1970).
[77]D. Bachelier et al., Phys. Lett. **B26**, 283 (1968); H. G. Pugh et al., Phys. Rev. Lett. **22**, 408 (1969); R. D. Plieninger et al., Nucl. Phys. **A137**, 20 (1969); J. R. Pizzi et al., ibid. **A136**, 496; P. Gaillard et al., Phys. Rev. Lett. **25**, 593 (1970); D. Bachelier et al., in [3b], p. 318; M. Jain et al., Nucl. Phys. **A153**, 49 (1970); B. Gottschalk and S. L. Kannenberg, Phys. Rev. **C2**, 24 (1970); A. Guichard et al., ibid. **C4**, 700 (1971); C. Jacquot et al., Nucl. Phys. **A148**, 325 (1970).
[78]I. A. Mackenzie et al., Nucl. Phys. **A178**, 225 (1971); J. C. Alder et al., Phys. Rev. **C6**, 18 (1972).
[79]Yu. P. Antuf'ev et al., ZhETF Pis. Red. **16**, 77 (1972) [JETP Lett. **16**, 52 (1972)].
[80]C. Tzara, Contribution to the International Seminar on Electromagnetic Interactions of Nuclei at Low and Medium Energies, Moscow, December 1972; G. Campos Venuti et al., Nucl. Phys. **A205**, 628 (1973); A. Bussiere et al., Contributed Papers of the 5th Intern. Conference on High Energy Physics and Nuclear Structure, Uppsala, June 1973, p. 170.
[81]M. Riou and Ch. Ruhla, Progr. Nucl. Phys. **2**, 195 (1969).
[82]J. Favier et al., Nucl. Phys. **A169**, 540 (1971).
[83]A. O. Agan'yants et al., ZhETF Pis. Red. **8**, 366 (1968) [JETP Lett. 8, 226 (1968)]; Phys. Lett. **B27**, 590 (1968); Nucl. Phys. **B11**, 79 (1969).
[84]Yu. D. Bayukov et al., Phys. Lett. **B33**, 416 (1970); in [15], p. 410; Yad. Fiz. **17**, 916 (1973) [Sov. J. Nucl. Phys. **17**, 479 (1973)].
[85]Yu. D. Bayukov et al., Annotatsii dokladov IV Mezhdunarodnoĭ konferentskii po fizike vysokikh énergiĭ i strukture yadra (Annotations of the Contributions to the 4th International Conference on High-Energy Physics and Nuclear Structure), Dubna, September 1971, Dubna, JINR, 1971, p. 70.
[86]Yu. D. Bayukov et al., Tezicy dokladov Vsesoyuznoĭ konferentsii "Yadernye reaktsii pri vysokikh énergiyakh" (Theses of the Contributions to the All-Union Union Conference "Nuclear Reactions at High Energies"), Tbilisi, July 1972, Moscow, FIAN SSSR, 1972, p. 44.
[87]S. Kullander et al., Phys. Lett. **B34**, 197 (1971); Nucl. Phys. **A173**, 357 (1971).
[88]Yu. R. Gismatullin and V. I. Ostroumov, Yad. Fiz. **11**, 285 (1970) [Sov. J. Nucl. Phys. **11**, 159 (1970)].
[89]E. Belotti, S. Bonetti, D. Cavalli and C. Matteuzzi, Nuovo Cimento **A14**, 567 (1973).
[90]V. V. Glagolev et al., JINR Preprint R1-6714, Dubna, 1972.
[91]C. F. Perdrisat et al., Phys. Rev. **187**, 1201 (1969).
[92]T. H. Tan, Phys. Rev. Lett. **23**, 359 (1969).
[93]A. E. Kudryavtsev, ZhETF Pis. Red. 14, 134 (1971) [JETP Lett. **14**, 90 (1971)].
[94]N. G. Birger et al., Yad. Fiz. 6, 344 (1967) [Sov. J. Nucl. Phys. **6**, 250 (1968)]; Yu. D. Bayukov et al., Phys. Lett. **B24**, 598 (1967); E. Coleman et al., Phys. Rev. Lett. **16**, 761 (1966); G. Bennet et al., ibid. **19**, 387 (1967); N. E. Booth et al., Phys. Rev. **D4**, 1261 (1971); V. I. Komarov et al., Yad. Fiz. **16**, 234 (1972) [Sov. J. Nucl. Phys. **16**, 129 (1973)]; J. C. Alder et al., Phys. Rev. **C6**, 2010 (1972).
[95]A. K. Kerman and L. S. Kisslinger, ibid. 180, 1483 (1969); J. S. Sharma et al., Nucl. Phys. B35, 466 (1971).

[96]L. Bertocchi and A. Capella, Nuovo Cimento 51, 359 (1967).
[97]V. M. Kolybasov and N. Ya. Smorodinskaya, Yad. Fiz. 17, 1211 (1973) [Sov. J. Nucl. Phys. 17, 630 (1973)]; Phys. Lett. B37, 272 (1971).
[98]N. C. Cragie and C. Wilkin, Nucl. Phys. B14, 477 (1969).
[99]T. Yao, Phys. Rev. 134, B454 (1964); S. Barshay, Phys. Rev. Lett. 17, 49 (1966).
[100]G. W. Barry, Ann. Phys. (N.Y.) 73, 482 (1972).
[101]P. Picozza et al., Nucl. Phys. A157, 190 (1970).
[102]V. A. Karmanov and L. A. Kondratyuk, Annotatsii dokladov Vsecoyuznoĭ konferentsii "Yadernye reaktsii pri vysokikh énergiyakh" (Annotations of the Contributions to the All-Union Conference "Nuclear Reactions at High Energies"), Tbilisi, June 1972, Moscow, Izd. FIAN, 1972, p. 81.
[103]M. P. Locher, Spring School on Pion Interactions at Low and Medium Energies, Lyceum Alpinum, 1971 (CERN Yellow Report 71-14, 1971, p. 155).
[104]D. S. Koltun, in [4], p. 201.
[105]E. H. S. Burhop, High Energy Physics, Vol. 3, N.Y., Academic Press, 1969.
[106]D. H. Wilkinson, Proc. Phys. Soc. 80, 997 (1962) [Russ. Transl., Usp. Fiz. Nauk 84, 451 (1964)].
[107]K. A. Brueckner et al., Phys. Rev. 84, 258 (1951); T. Ericson, Phys. Lett. 2, 278 (1962).
[108]H. Davies, H. Muirhead and J. N. Woulds, Nucl. Phys. 78, 667 (1966).
[109]D. M. Lee, R. C. Minehart, S. E. Sobottka and K. Ziock, ibid. A182, 20 (1972).
[110]V. M. Kolybasov and V. A. Tsepov, Yad. Fiz. 14, 744 (1971) [Sov. J. Nucl. Phys. 14, 418 (1972)].
[111]V. M. Kolybasov, Yad. Fiz. 3, 729 (1966) [Sov. J. Nucl. Phys. 3, 535 (1966)].
[112]V. S. Demidov, V. S. Verebryusov, V. G. Kirillov-Ugryumov et al., Zh. Eksp. Teor. Fiz. 46, 1220 (1964) [Sov. Phys.-JETP 19, 826 (1964)].
[113]A. O. Vaĭsenberg, É. D. Kolganova and N. V. Rabin, ibid. 47, 1262 (1964)[20, 854 (1965)].
[114]Yu. G. Budyashev, V. G. Zinov et al., Zh. Eksp. Teor. Fiz. 62, 21 (1972) [Sov. Phys.-JETP 35, 13 (1972)].
[115]I. S. Shapiro and V. M. Kolybasov, Zh. Eksp. Teor. Fiz. 44, 270 (1963) [Sov. Phys.-JETP 17, 185 (1963)].
[116]V. M. Kolybasov, Yad. Fiz. 3, 965 (1966) [Sov. J. Nucl. Phys. 3, 704 (1966)].
[117]D. M. Lee, R. C. Minehart, S. E. Sobottka and K. H. Ziock, Nucl. Phys. A197, 106 (1972).
[118]V. M. Kolybasov and T. A. Lomonosova, Yad. Fiz. 11, 578 (1970) [Sov. J. Nucl. Phys. 11, 325 (1970)].
[119]Yu. A. Batusov, S. A. Bunyatov, V. M. Sidorov et al., JINR Preprint R1-4309, Dubna, 1969.
[120]G. Backenstoss, Ann. Rev. Nucl. Sci. 20, 467 (1970) [Russ. Transl., Usp. Fiz. Nauk 107, 405 (1972)].
[121]P. A. Katz, K. Bunnell et al., Phys. Rev. D1, 1267 (1970).
[122]D. H. Davies, S. P. Lovell et al., Nucl. Phys. B1, 434 (1967).
[123]W. A. Bardeen and E. Wayne Torigoe, Phys. Lett. B38, 135 (1972).
[124]V. R. Veirs and R. A. Burnstein, Phys. Rev. D1, 1883 (1970).
[125]M. Nicolic, Y. Eisenberg et al., Helv. Phys. Acta 33, 221 (1960).
[126]E. H. S. Burhop et al., Nucl. Phys. A132, 625 (1969); E. H. S. Burhop, ibid. B44, 445 (1972).
[127]H. Bethe, Ann. Rev. Nucl. Sci. 21, 93 (1971).
[128]C. E. Wiegand, Phys. Rev. Lett. 22, 1235 (1969).
[129]T. Ericson and F. Scheck, Nucl. Phys. B19, 450 (1970).
[130]G. Backenstoss, A. Bamberger et al., Phys. Lett. B38, 181 (1972).
[131]B. W. Allardyce, C. J. Batty, D. J. Baugh et al., ibid. B41, 577.

Translated by N. M. Queen